Electronic Supplementary Material (ESI) for Medicinal Chemistry Communications.

Discovery of mitochondria-targeting berberine derivatives as inhibitors of proliferation, invasion and migration against rat C6 and human U87 glioma cells

Shengnan Fu,[†,‡,¶] Yanqi Xie,[†,‡] Jue Tuo,[†] Yalong Wang,[†] Wenbo Zhu,[§] Sihan Wu,[§] Guangmei Yan,[*§] Haiyan Hu,[*†]

[†]School of Pharmaceutical Sciences, Sun Yat-sen University, Waihuan East Road 132, Guangzhou 510006, China

[§]Department of Pharmacology, Zhongshan School of Medicine, Sun Yat-sen University, Zhongshan II Road 74, Guangzhou 510080, China

[¶]Department of Pharmacy, The People's Hospital of ZhongShan, Sunwen East Road 2, Zhongshan 528403, China

* Corresponding authors, Dr. Haiyan Hu and Dr.Guangmei Yan

Tel: +86-020-39343118; Fax: +86-020-39343118

E-mail: lsshhy@mail.sysu.edu.cn (Hu); ygm@mail.sysu.edu.cn (Yan)

[‡]These authors contributed equally.

1. Materials and Methods

1.1. General

Berberine hydrochloride (Purity: > 97%) was purchased from Xi'an Xiaocao Botanical Development Co., Ltd (Shaanxi, China) and dried under vacuum before use. Other reagents and solvents (Analytical grade) from Aladdin (Shanghai, China) were used without further purification. Silica gel (GF254) based thin-layer chromatography was used to monitor the processes of reactions. NMR spectra were measured on a Bruker Avance III 400 MHz spectrometer. Chemical shifts were recorded in parts per million (ppm) using tetramethylsilane as an internal standard in CD_3OD or DMSO. Electrospray ionization-mass spectrometry (ESI-MS) was used to acquire the mass spectra on a TSQ Quantum Access Max (Thermo Scientific, San Jose, CA, USA) in positive mode. High-performance liquid chromatography (HPLC) (Agilent 1200, USA) was performed to determine the purity of the compounds described in this paper (Column, Waters C_{18}, 250×4.6 mm, 5 μm; eluent, aqueous formic acid solution (0.25 M, pH 2.8)/ acetonitrile (65:35); injection volume, 20 μL； flow, 1 mL min^{-1}; detector, UV detector; ultraviolet detected wavelength, 344 nm). The ultraviolet absorption spectra of berberine and its derivatives are characterized by three absorbance peaks centered around 230 nm, 267 nm and 344 nm in the region of 190-400 nm (HPLC, UV detector, full scan mode of the DAD mode). The purity of the berberine derivatives was found to be greater than 95%.

1.2. Procedure for preparation of 9-O-substituted berberine derivatives [28]

*1.2.1. Synthesis of berberrubine (**2**)*

Under nitrogen protection, anhydrous berberine hydrochloride (10.0 g, 26.9 mmol) was suspended in decalin (250 mL) and pyrolyzed at 190 ℃ for 5 h. The reaction mixture was concentrated by a rotary evaporator to afford a crude residue that was purified by neutral alumina column chromatography (Dichloromethane/ methanol 100:1) to furnish pure red crystal **2** (87% yield); ^{1}H NMR (400 MHz, CD_3OD) δ: 9.22 (s, 1H), 7.96 (s, 1H), 7.48 (d, J = 8.2 Hz, 1H), 7.39 (s, 1H), 6.83 (d, J = 8.3 Hz, 1H), 6.81 (s, 1H), 6.02 (s, 2H), 4.52-4.62 (t, J = 6.3 Hz, 2H), 3.86 (s, 3H), 3.05-3.14 (t, J = 6.3 Hz, 2H); ^{13}C NMR (101 MHz, CD_3OD) δ: 151.11, 150.85, 149.47, 147.31, 135.54, 133.74, 130.66, 124.21, 122.90, 121.71, 119.63,

109.20, 108.17, 105.81, 103.25, 56.79, 55.53, 28.96; ESI-MS *m/z*: 322 $[M+H]^+$.

*1.2.2. 9-O-decyl-berberine (**3a**)*

The resulting pure **2** (0.32 g, 1 mmol) was dissolved in 5 mL DMF, to which 1-bromodecane (0.827 mL, 4 mmol) was added. The mixture was stirred at 80 ℃ for 12 h, and filtrated to give the crude residue that was purified by neutral alumina column chromatography (Dichloromethane/methanol, 200-100:1) to provide pure yellow crystal **3a** (70-80% yield); ^{1}H NMR (400 MHz, DMSO) δ 9.74 (s, 1H), 8.93 (s, 1H), 8.18 (d, J = 8.8 Hz, 1H), 7.98 (d, J = 9.1 Hz, 1H), 7.78 (s, 1H), 7.08 (s, 1H), 6.16 (s, 2H), 4.94 (t, J = 6.3 Hz, 2H), 4.26 (t, J = 6.7 Hz, 2H), 4.04 (s, 3H), 3.20 (t, J = 6.7 Hz, 2H), 1.91-1.81 (m, 2H), 1.45 (d, J = 7.3 Hz, 2H), 1.24 (s, 12H), 0.84 (d, J = 6.8 Hz, 3H); ^{13}C NMR (101 MHz, DMSO) δ: 150.34, 149.72, 147.59, 145.23, 142.82, 137.32, 132.99, 130.57, 126.57, 123.27, 121.59, 120.38, 120.19, 108.33, 105.39, 102.03, 74.21, 56.99, 55.24, 31.26, 29.45, 28.96, 28.81, 28.67, 26.29, 25.23, 22.05, 13.90; ESI-MS *m/z*: 462 $[M-Br]^+$.

*1.2.3. 9-O-dodecyl-berberine (**3b**)*

As indicated in the synthesis of **3a**, the same procedure was followed to produce yellow crystal **3b** (70-80% yield); ^{1}H NMR (400 MHz, DMSO) δ: 9.76 (s, 1H), 8.95 (s, 1H), 8.19 (d, J = 9.1 Hz, 1H), 7.99 (d, J = 9.1 Hz, 1H), 7.80 (s, 1H), 7.09 (s, 1H), 6.17 (s, 2H), 4.91 (t, J = 6.7 Hz, 2H), 4.28 (t, J = 6.7 Hz, 2H), 4.05 (s, 3H), 3.24 (t, J = 6.7 Hz, 2H), 1.81-1.94 (m, 2H), 1.42-1.52 (m, 2H), 1.39-1.22 (m, 16H), 0.85 (t, J = 6.7 Hz, 3H); ^{13}C NMR (101 MHz, DMSO) δ: 150.34, 149.76, 147.62, 145.20, 142.84, 137.36, 133.01, 130.58, 126.62, 123.26, 121.61, 120.37, 120.16, 108.35, 105.38, 102.03, 74.22, 57.00, 55.30, 31.23, 29.43, 28.97, 28.77, 28.65, 26.30, 25.21, 22.03, 13.87; ESI-MS m/z: 490 $[M-Br]^+$.

*1.2.4. 9-O-cetyl-berberine (**3c**)*

The procedure for synthesizing **3a** was also performed to afford yellow crystal **3c** (70-80% yield); ^{1}H NMR (400 MHz, DMSO) δ: 9.75 (s, 1H) 8.94 (s, 1H), 8.20 (d, J = 8.9 Hz, 1H), 8.00 (d, J = 8.9 Hz, 1H), 7.80 (s, 1H), 7.09 (s, 1H), 6.18 (s, 2H), 4.95 (t, J = 6.7 Hz, 2H), 4.29 (t, J = 6.7 Hz, 2H), 4.05 (s, 3H), 3.23 (t, J = 6.7 Hz, 2H), 1.87-1.96 (m, 2H), 1.48-1.58 (m,

2H), 1.24 (s, 24 H), 0.85 (t, J = 3.4 Hz, 3H); ^{13}C NMR (101 MHz, DMSO) δ: 150.36, 149.78, 147.65, 145.23, 142.86, 137.40, 133.02, 130.62, 126.68, 123.24, 121.63, 120.40, 120.18, 108.36, 105.39, 102.05, 74.21, 57.01, 55.29, 31.23, 29.43, 28.99, 28.78, 28.64, 26.31, 25.22, 22.03, 13.87; ESI-MS *m/z*: 546 $[M\text{-}Br]^+$.

*1.2.5. 9-O-octadecyl-berberine (**3d**)*

Except the reaction time was 24 h, the similar process in preparation of **3a** was utilized to synthesize yellow crystal **3d** (70-80% yield); ^{1}H NMR (400 MHz, DMSO) δ: 9.75 (s, 1H), 8.94 (s, 1H), 8.19 (d, J = 9.0 Hz, 1H), 8.00 (d, J = 9.0 Hz, 1H), 7.80 (s, 1H), 7.09 (s, 1H), 6.17 (s, 2H), 4.95 (t, J = 6.4 Hz, 2H), 4.28 (t, J = 6.4 Hz, 2H), 4.05 (s, 3H), 3.23 (t, J = 5.3 Hz, 2H), 1.83-1.92 (m, 2H), 1.42-1.52 (m, 2H), 1.39 – 1.25 (m, 28H), 0.86 (t, J = 4.9 Hz, 3H); ^{13}C NMR (101 MHz, DMSO) δ: 150.37, 149.80, 147.66, 145.22, 142.87, 137.44, 133.03, 130.63, 126.70, 123.26, 121.65, 120.40, 120.18, 108.37, 105.39, 102.04, 74.22, 57.01, 55.30, 31.21, 29.41, 28.95, 28.75, 28.62, 26.31, 25.21, 22.01, 13.87; ESI-MS *m/z*: 574 $[M\text{-}Br]^+$.

*1.2.6. 9-O-benzyl-berberine (**3e**)*

The same procedure as described in synthesis of **3a** was adopted other than shortening the reaction time to 2 h to give yellow crystal **3e** (70-80% yield); ^{1}H NMR (400 MHz, DMSO) δ: 9.73 (s, 1H), 8.93 (s, 1H), 8.21 (d, J = 9.1 Hz, 1H), 8.00 (d, J = 9.0 Hz, 1H), 7.78 (s, 1H), 7.59 (d, J = 7.3 Hz, 2H), 7.38 (dt, J = 8.5, 5.1 Hz, 3H), 7.08 (s, 1H), 6.17 (s, 2H), 5.36 (s, 2H), 4.91 (t, J = 6.7 Hz, 2H), 4.08 (s, 3H), 3.21 (t, J = 6.7 Hz, 2H); ^{13}C NMR (101 MHz, DMSO) δ: 150.66, 149.78, 147.63, 145.24, 141.95, 137.30, 136.40, 132.89, 130.57, 128.75, 128.37, 128.31, 126.49, 123.71, 121.77, 120.32, 120.15, 108.36, 105.39, 102.04, 75.32, 57.03, 55.33, 26.31; ESI-MS *m/z*: 412 $[M\text{-}Br]^+$.

1.3. Preparation of 13-substituted berberine derivatives

*1.3.1 Synthesis of dihydroberberine (**4**)* [29, 30]

Anhydrous berberine hydrochloride (6.0 g, 16.1 mmol) was suspended in pyridine (50 mL), followed by addition of sodium borohydride (700 mg, 18.5 mmol) very slowly under stirring at room temperature. After ice water (200 mL) was added to the reaction system and

subsequent filtration, the filter cake was dried under vacuum to give the intermediate **4**; ESI-MS *m/z*: 338 $[M+H]^+$.

*1.3.2. 13-decyl-berberine (**5f**)*[31]

Anhydrous intermediate **4** (0.34 g, 1 mmol), 1-bromodecane (0.827 mL, 4 mmol) and sodium iodide (0.6 g, 4 mmol) were placed in a thick-walled three-necked flask together with anhydrous acetonitrile (20 mL). Then the flask was heated under nitrogen protection with stirring at 80 ℃ for 12 h followed by filtration. The obtained filtrate was concentrated and purified by a three-step column chromatography, neutral alumina column chromatography (Petroleum ether/*n*-butanol, 10:1), column chromatography on silica gel (*n*-butanol/water/acetic acid, 50:3:3), Sephadex™ LH-20 column chromatography (Methanol). The synthesis of **5g**, **5h** and **5i** followed the same procedure as **5f**.

Yellow crystal **5f**, yield: 15%. ^{1}H NMR (400 MHz, DMSO) δ: 9.90 (s, 1H), 8.21 (s, 2H), 7.31 (s, 1H), 7.17 (s, 1H), 6.20 (s, 2H), 4.81 (t, J = 5.6Hz, 2H), 4.11 (s, 3H), 4.10 (s, 3H), 3.34 (m, 2H), 3.09 (t, J = 5.6Hz, 2H), 1.74 (m, 2H), 1.38 (m, 2H), 1.24 (m, 12H), 0.87 (t, J = 6.6 Hz, 3H); ^{13}C NMR (101 MHz, DMSO) δ: 150.69, 149.49, 147.03, 144.90, 144.78, 136.24, 134.65, 134.56, 132.68, 126.41, 121.91, 121.71, 120.78, 109.58, 108.85, 102.60, 62.54, 57.49, 31.76, 30.88, 29.41, 29.12, 28.90, 27.87, 22.55, 14.43. ESI-MS *m/z*: 476 $[M-I]^+$.

*1.3.3. 13-dodecyl-berberine (**5g**)*

Yellow crystal **5g**, yield: 10%. ^{1}H NMR (400 MHz, DMSO) δ: 9.92 (s, 1H), 8.20 (s, 2H), 7.29 (s, 1H), 7.16 (s, 1H), 6.18 (s, 2H), 4.81 (t, J = 5.6Hz, 2H), 4.10 (s, 3H), 4.09 (s, 3H), 3.34 (m, 2H), 3.08 (t, J = 5.6Hz, 2H), 1.75 (m, 2H), 1.37 (m, 2H), 1.23 (m, 16H), 0.85 (m, 3H); ^{13}C NMR (101 MHz, DMSO) δ: 150.69, 149.50, 147.04, 144.81, 144.75, 136.51, 136.26, 134.69, 134.53, 132.70, 126.39, 121.91, 121.71, 120.78, 109.60, 108.83, 102.59, 62.51, 57.47, 31.76, 30.86, 29.47, 29.44, 29.40, 29.16, 29.06, 28.88, 27.87, 22.56. ESI-MS *m/z*: 504 $[M-I]^+$.

*1.3.4. 13-cetyl-berberine (**5h**)*

Yellow crystal **5h**, yield: 10%. ^{1}H NMR (400 MHz, DMSO) δ: 9.90 (s, 1H), 8.20 (s, 2H), 7.29 (s, 1H), 7.16 (s, 1H), 6.18 (s, 2H), 4.80 (t, J = 5.6Hz, 2H), 4.10 (s, 3H), 4.09 (s, 3H), 3.34

(s, 2H), 3.08 (m, 2H), 1.77 – 1.71 (m, 2H), 1.36 (m, 2H), 1.23 (s, 24H), 0.86 (t, J = 5.8 Hz, 3H). ^{13}C NMR (101 MHz, DMSO) δ: 150.16, 148.98, 146.51, 144.29, 135.70, 134.09, 134.01, 132.17, 131.65, 131.40, 128.57, 125.88, 121.31, 121.19, 120.22, 108.99, 108.31, 102.06, 61.98, 56.94, 31.24, 30.38, 29.96, 29.00, 28.96, 28.65, 28.61, 28.40, 22.03, 18.59, 13.83, 13.45.ESI-MS *m/z*: 560 $[M-I]^+$.

*1.3.5. 13-octadecyl-berberine (**5i**)*

Yellow crystal **5i**, yield: 10%. ^{1}H NMR (400 MHz, DMSO) δ: 9.90 (s, 1H), 8.20 (s, 2H), 7.29 (s, 1H), 7.16 (s, 1H), 6.18 (s, 2H), 4.80 (s, 2H), 4.10 (s, 3H), 4.09 (s, 3H), 3.24 (d, J = 7.8 Hz, 2H), 3.08 (s, 2H), 1.83 – 1.70 (m, 2H), 1.37 (m, 2H), 1.23 (s, 28H), 0.85 (t, J = 6.8 Hz, 3H). ^{13}C NMR (101 MHz, DMSO) δ: 150.67, 149.49, 147.03, 144.81, 144.74, 136.25, 134.67, 134.52, 132.68, 126.38, 121.89, 121.70, 120.76, 109.58, 108.82, 102.58, 62.50, 57.47, 31.75, 30.87, 29.48, 29.16, 27.87, 22.55, 14.41. ESI-MS *m/z*: 588 $[M-I]^+$.

*1.3.6. 13-benzyl-berberine (**5j**)*

The preparation of **5j** followed the procedure in synthesizing **5g** except that the reaction time was 5 h. Yellow crystal **5j**, yield: 37%. ^{1}H NMR (400 MHz, DMSO) δ: 10.06 (s, 1H), 8.11 (d, J = 9.2 Hz, 1H), 7.80 (d, J = 9.3 Hz, 1H), 7.38 (t, J = 7.3 Hz, 2H), 7.31 (d, J = 7.1 Hz, 1H), 7.18 (s, 3H), 6.98 (s, 1H), 6.09 (s, 2H), 4.90 (s, 2H), 4.76 (s, 2H), 4.13 (s, 3H), 4.04 (s, 3H), 3.17 (s, 2H). ^{13}C NMR (101 MHz, DMSO) δ: 150.69, 149.69, 146.88, 145.99, 144.74, 139.63, 137.64, 134.55, 133.23, 130.48, 129.57, 128.49, 127.27, 126.64, 122.15, 121.74, 120.49, 108.97, 108.60, 102.53, 62.55, 57.41, 35.98, 27.76. ESI-MS *m/z*: 426 $[M-I]^+$.

1.4. Determination of Log P values

The traditional saturation shake flask methods were utilized to measure the log P values of compounds **1**, **3a-e** and **5f-j**. Briefly, *n*-octanol and doubly distilled water with the same volume were placed in a conical flask and shaken at 100 times per minute at 37 ℃. After 24 h, the mixture was centrifuged at 4000 rpm for 10 min and separated to obtain the *n*-octanol-saturated water and water-saturated *n*-octanol.

Compounds **1**, **3a-e** and **5f-j** (1 mg) were dissolved in water-saturated *n*-octanol (4 mL),

respectively, followed by addition of *n*-octanol-saturated water (4 mL). The mixtures were shaken at 100 times per minute at 37 ℃ for 24 h, centrifuged at 4000 rpm for 10 min and separated to obtain aqueous phases and oil phases. Precise volumes of both phases were transferred to volumetric flasks, diluted and the concentrations of **1**, **3a-e** and **5f-j** were determined by HPLC as described above. The partition coefficients (P) were reported as the logarithm of P (Log *P*). In addition, the standard curves of **1**, **3a-e** and **5f-j** were constructed by dissolving compounds in methanol at the concentration range of 0.05-10 μg/mL with the r^2 value of > 0.9995.

1.5. Biology

Rat C6 and human U87 glioma cells were obtained from the American Type Culture Collection (Manassas, VA) and cultured in Dulbecco's modified Eagle's medium (DMEM, Invitrogen, Grand Island, NY) containing 10% fetal bovine serum (FBS), penicillin (100 IU mL^{-1}) and streptomycin (100 μg mL^{-1}) in an atmosphere of 5% CO_2 at 37 ℃. Compounds **1**, **3a-e** and **5f-j** were dissolved in sterile DMSO at 1 mM and stored at – 4 ℃. They were diluted by aseptic culture medium to indicated concentrations immediately before their use.

1.5.1. Cell proliferation inhibition assays

Cell viability was measured by MTT assay. C6 or U87 glioma cells were seeded in 96-well plates at a density of 5000 cells/well and cultured for 24 h at 37 ℃. Cells were then treated with compounds **1**, **3a-e** and **5f-j** for 24 h, followed by incubation with 10 μL of MTT (5.0 mg mL-1, Sigma-Aldrich, St. Louis, MO) for 4 h at 37 ℃. After removing the culture medium, the reduced MTT dye was solubi1ized by 100 μL of DMSO and the absorbance at 570 nm ($A_{540\ nm}$) was read on an EXL800 microimmunoanalyser (BioTek, Burlington, VT). The cell viability = $A_{540\ nm}$ for the treated cells/$A_{540\ nm}$ for the control cells × 100%.

1.5.2. In vitro migration and invasion assays

Cell migration and invasion were performed on Milicell hanging cell culture inserts with 8-μm pore size polycarbonate membrane (Millipore Corporation, Billerica, MA). For migration assay the inserts were not precoated by matrigel (BD Biosciences, Bedford, MA) while for

invasion assay the inserts were precoated by matrigel pursuant to the manufacturer's instructions. After C6 or U87 cells were trypsinized and resuspended in medium free of FBS, they were seeded in serum-free DMEM in the upper chamber in the presence of synthetic derivatives, with 600 μL medium with 10% FBS in the lower chamber. Simultaneously, an equal number of C6 or U87 cells of each group were placed in 96-well plates to determine the total cell number by MTT assay. Densities of 2.5×10^4 and 5×10^4 cells/well were used for migration and invasion assay, respectively. Following 24 h incubation at 37 ℃, the cells in the upper chamber were removed. Cells attached on the under surface of the polycarbonate membrane were fixed with 4% polyoxymethylene for 30 min, stained with 0.2% crystal violet for 10 min, washed with PBS and photographed to obtain five random fields (× 200). The relative migration or invasion of cells were represented as percentage of average migrated or invaded cell numbers in the control group, respectively.

1.5.3. Subcellular localization

A laser confocal microscope (LSM 710, Carl Zeiss, Germany) was employed to study the subcellular localization of synthetic analogues on live C6 and U87 cells using Mitotracker Green FM (Invitrogen, Grand Island, NY). Briefly, C6 or U87 cells were seeded in culture dishes with microscope slides in the bottom at a density of 4×10^4 overnight. After further incubation with 1 μL compounds **1**, **3b**, **3c**, **5g** and **5h** for 24 h, the medium was removed followed by washing with PBS (pH 7.4) three times. Then the cells were stained in culture medium containing 500 nM of Mitotracker Green FM at 37 ℃ for 37 min, washed by cold PBS three times and photographed at the × 100 oil immersion objective. These berberine derivatives have yellow fluorescence with peak mission around 550 nm. Green and yellow fluorescence were collected and then superimposed.

1.5.4. Measurement of reactive oxygen species

Fluorescent dye dihydroethidium (DHE, Ex/Em = 518 nm/605 nm, Invitrogen Molecular Probes) was employed to determine the intracellular ROS levels of C6 and U87 tumor cells after incubation with or without compounds **1**, **3a-e** and **5f-j**. Briefly, C6 or U87 glioma cells were seeded in culture dishes (35 mm) at a density of 20000 cells/dish and cultured for 24 h in 5% CO_2 at 37 ℃. Whereafter, cells were treated with compounds **1**, **3a-e** and **5f-j** (2 μL)

for 24 h, followed by removing the culture medium and incubation with DHE (2.5 μL) for 20 min in 5% CO_2 at 37 ℃. After the cells were washed with DMEM three times, red fluorescence was detected by an inverted fluorescent microscope (IX71, Olympus Inc., Japan).

1.5.5. Prediction of BBB penetration

According to the Lipinski's rules, we evaluated the 'drug-like-quality' and brain penetration ability of the representative compounds (**1**, **3a**, **3b**, **5f**, **5g**) by the calculation of log BB via the equation of log BB = -0.0148 × PSA + 0.152× clogP + 0.130 as criteria [32]. Log BB (log (C_{brain}/C_{blood})) means the ratio of the steady-state concentrations of the drug molecule in the brain and in the blood; PSA (polar surface area) and clogP were calculated by the Molinspiration desktop property calculator (Molinspiration Cheminformatics, Slovak Republic). As for the criteria, compounds with log BB > 0.3 can cross the BBB readily, while compounds with log BB < -1.0 are only poorly distributed to the brain [33].

Statistics Experiments were performed in triplicate and repeated at least three times. Data were presented as mean ± SD and compared by one-way analysis of variance followed by post hoc tests including with the Bonferroni correction to determine the significance among groups in SPSS17.0 (v17.0; SPSS, Inc, Chicago, IL, USA). The significant level was $p < 0.05$

2. Nuclear magnetic resonance (NMR) spectra of compounds **1**, **3a-e** and **5f-j**.

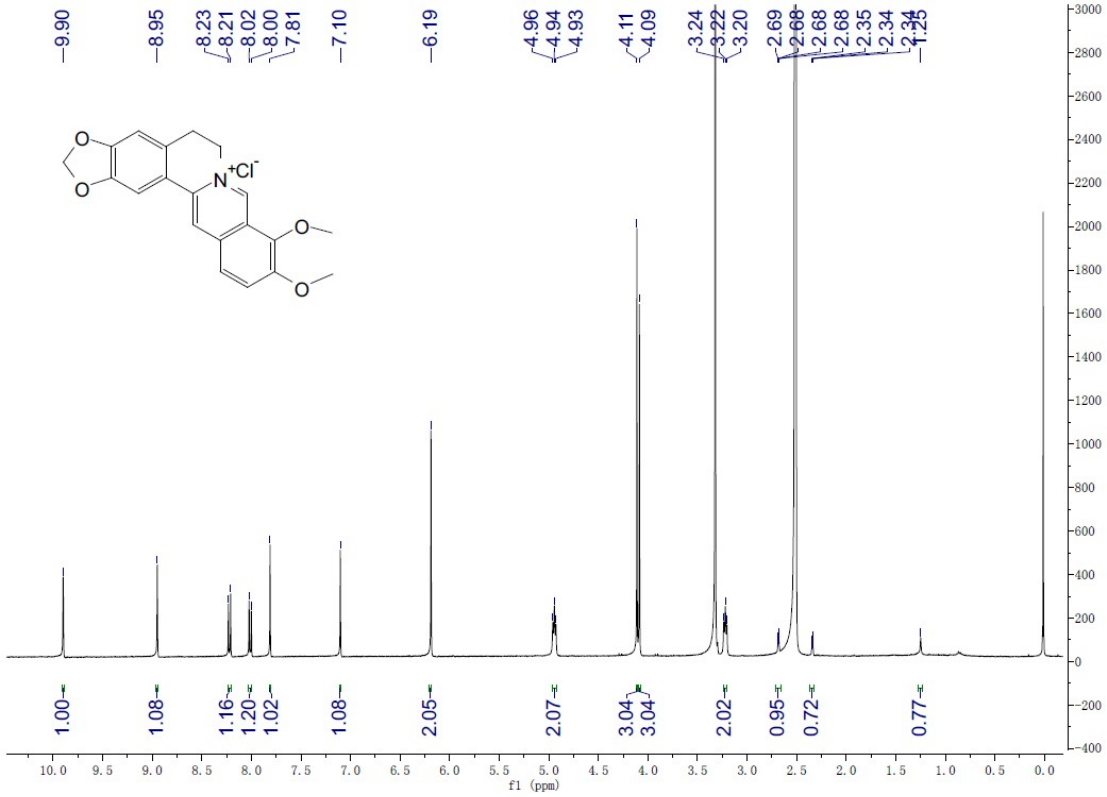

Fig.1. ^{1}H NMR, Berberine

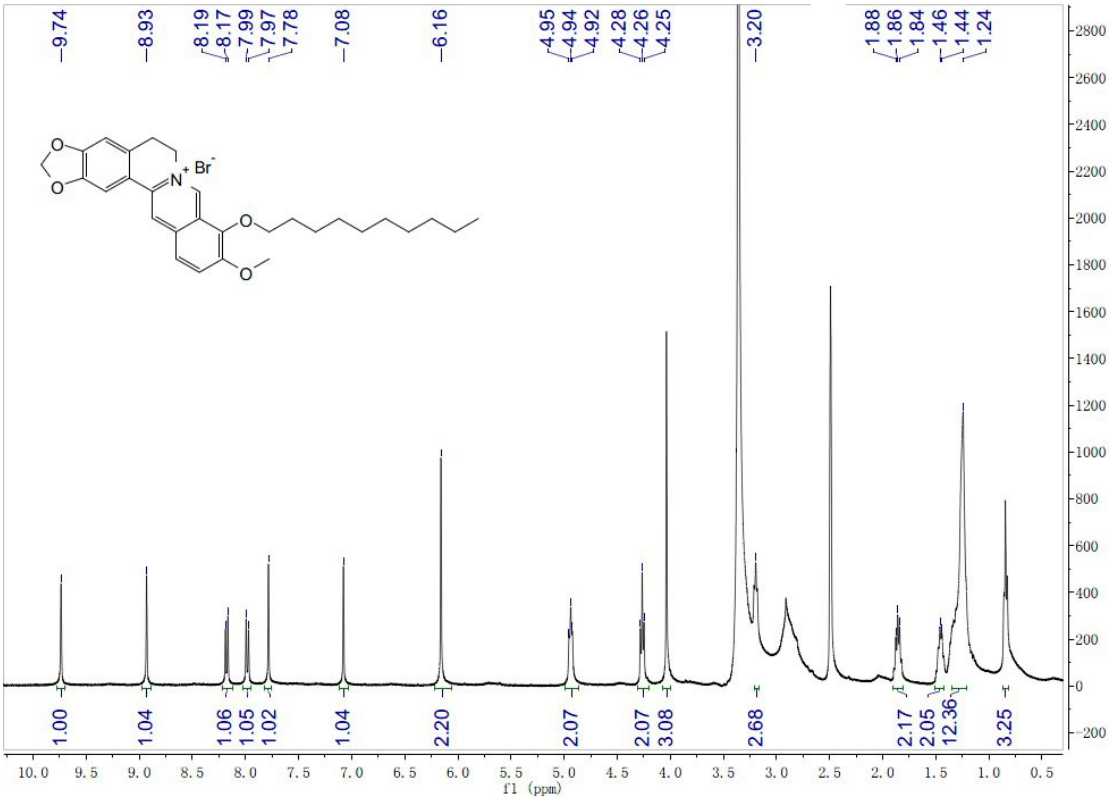

Fig.2. [1]H NMR, 9-*O*-decyl-berberine (**3a**)

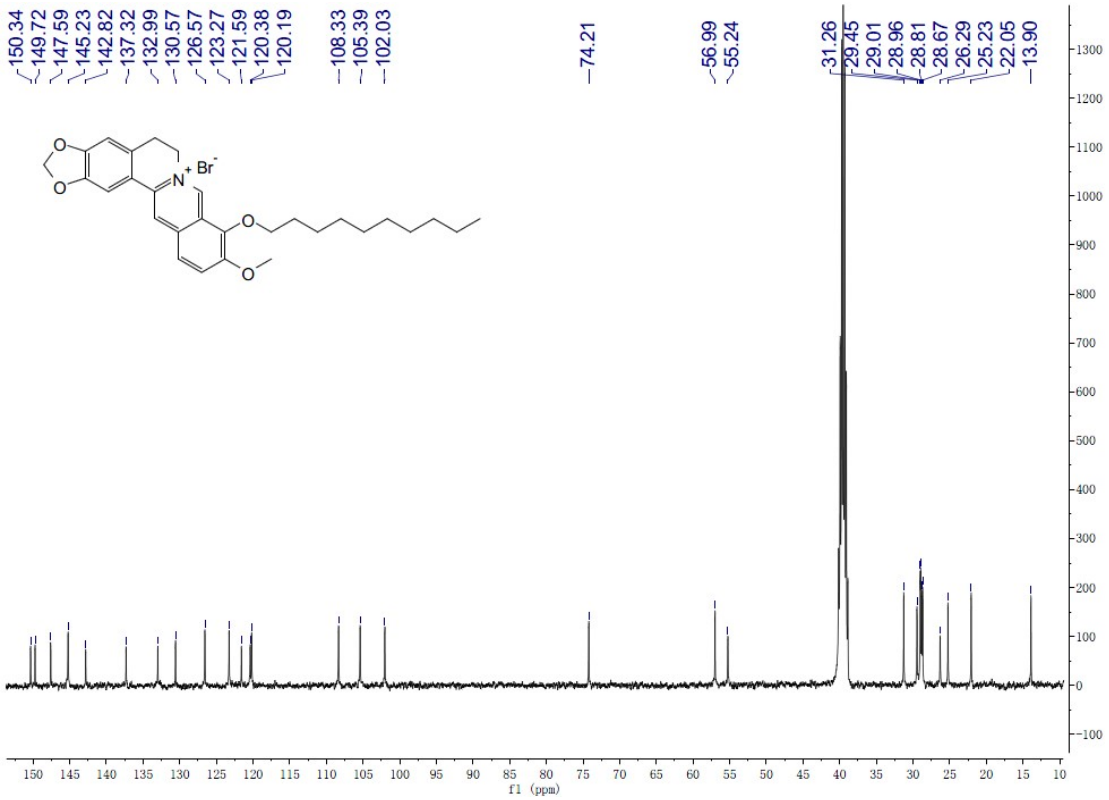

Fig.3. [13]C NMR, 9-*O*-decyl-berberine (**3a**)

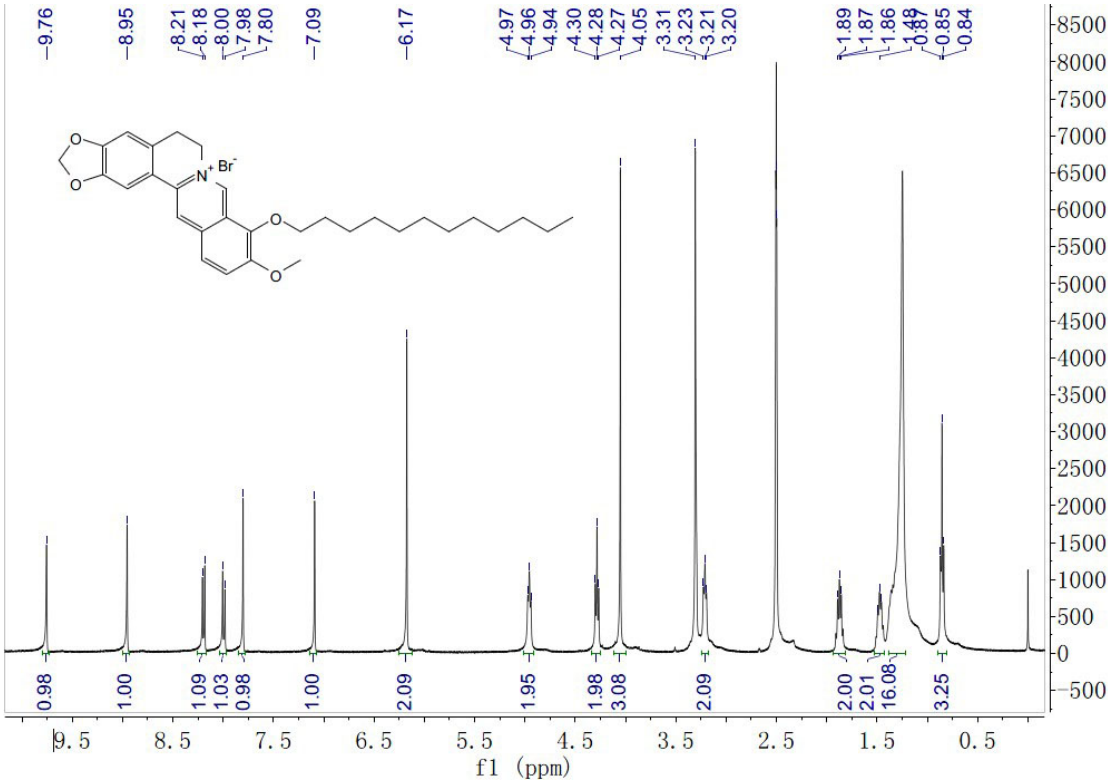

Fig.4. [1]H NMR, 9-*O*-dodecyl-berberine (**3b**)

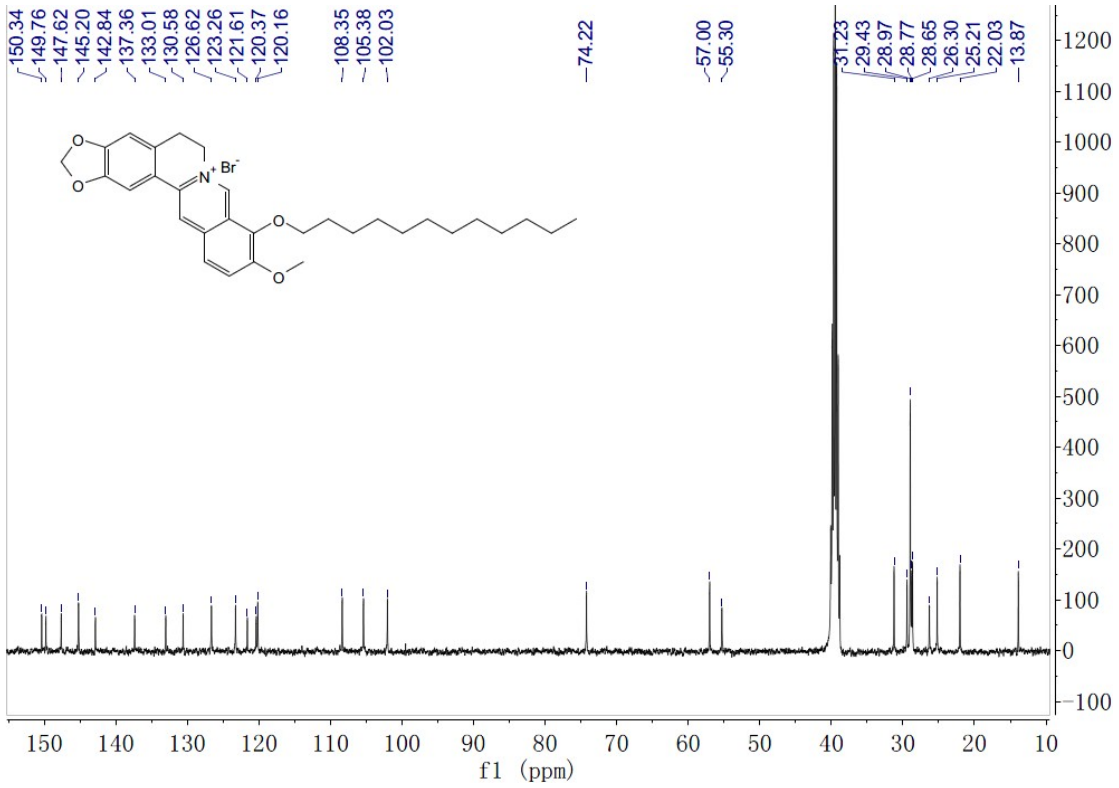

Fig.5. ^{13}C NMR, 9-*O*-dodecyl-berberine (**3b**)

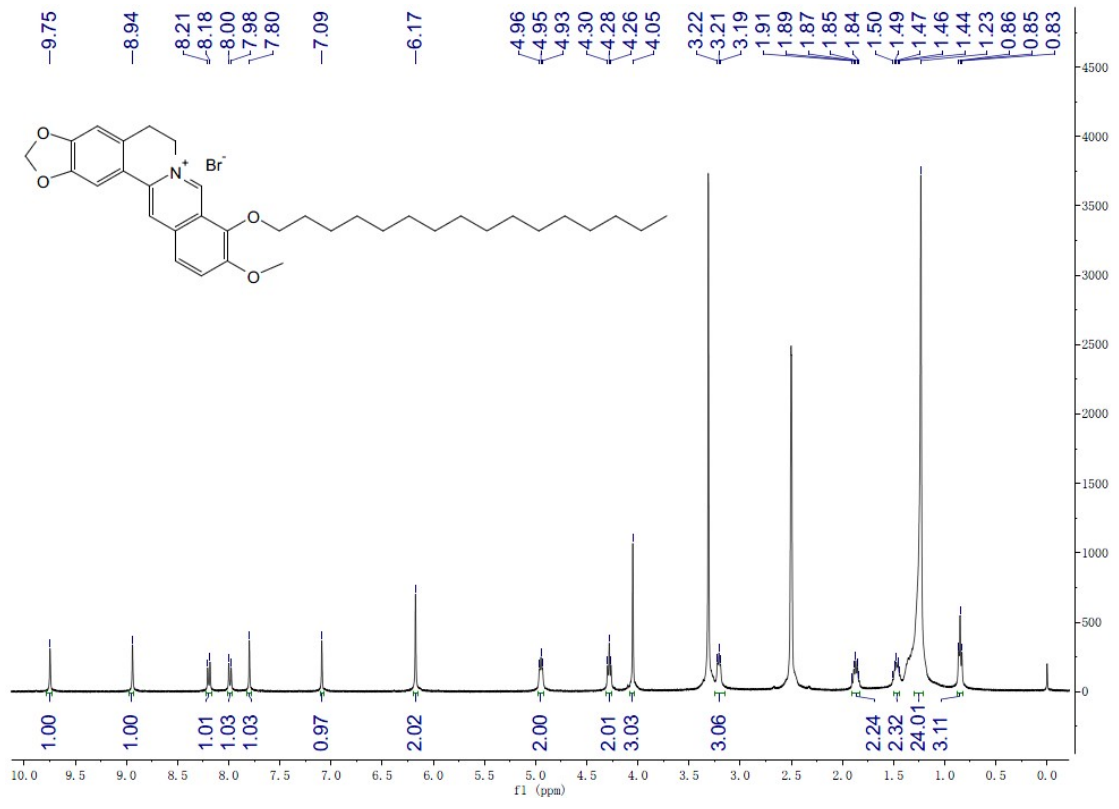

Fig.6. ^{1}H NMR, 9-*O*-cetyl-berberine (**3c**)

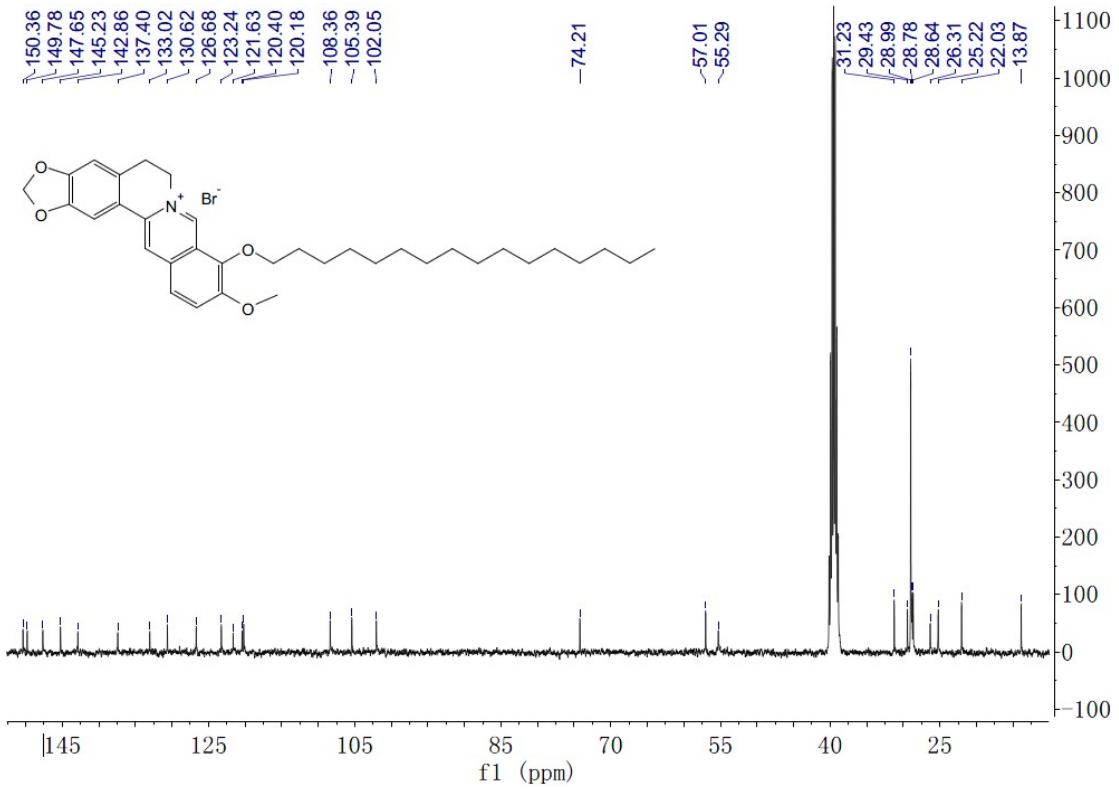

Fig.7. ^{13}C NMR, 9-*O*-cetyl-berberine (**3c**)

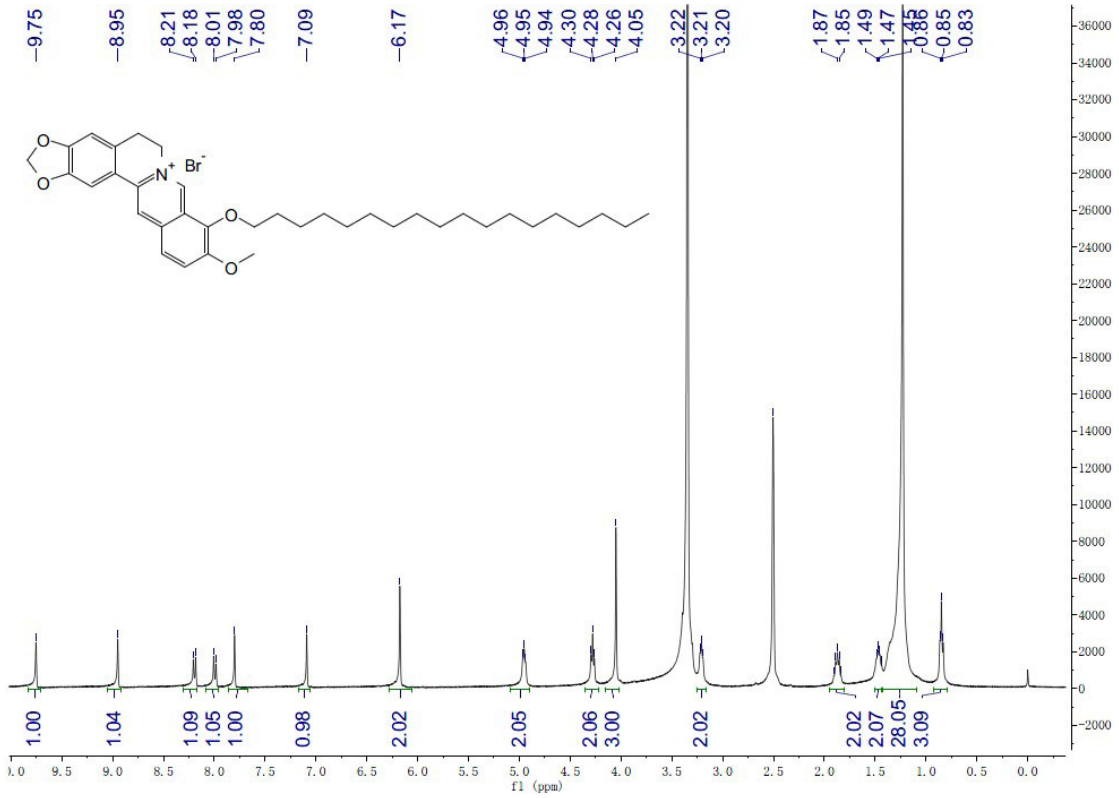

Fig.8. ^{1}H NMR, 9-*O*-octadecyl-berberine (**3d**)

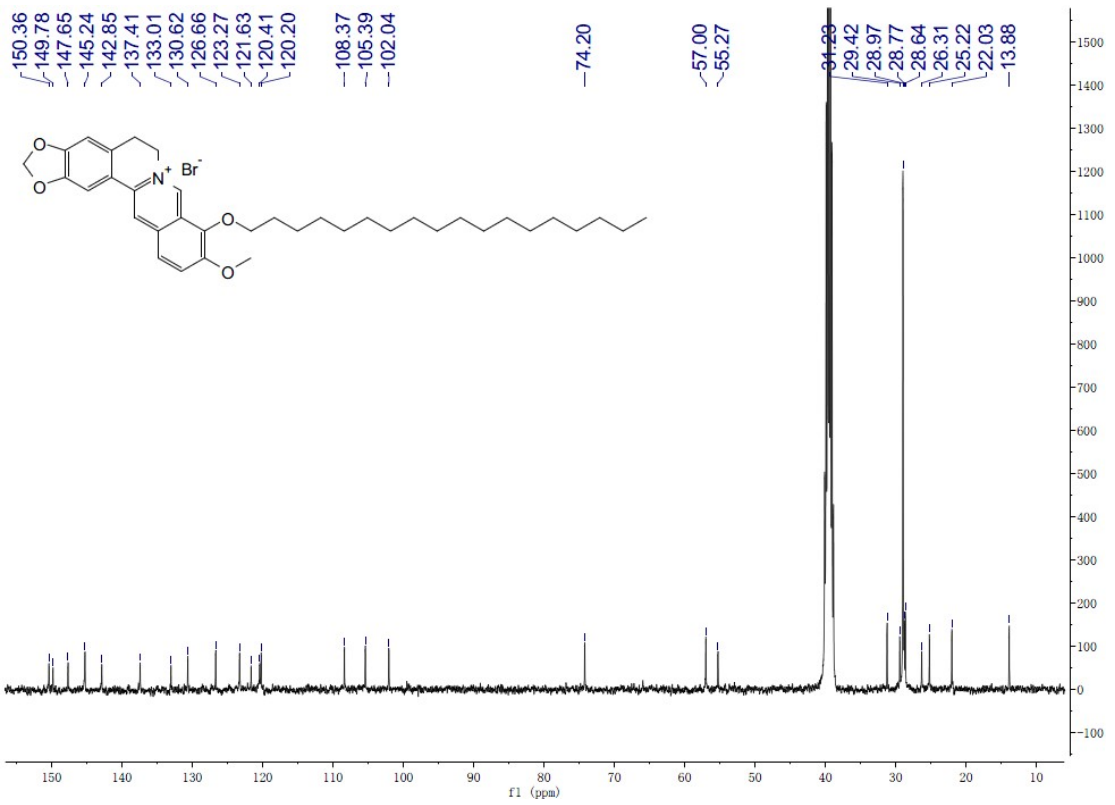

Fig.9. ^{13}C NMR, 9-*O*-octadecyl-berberine (**3d**)

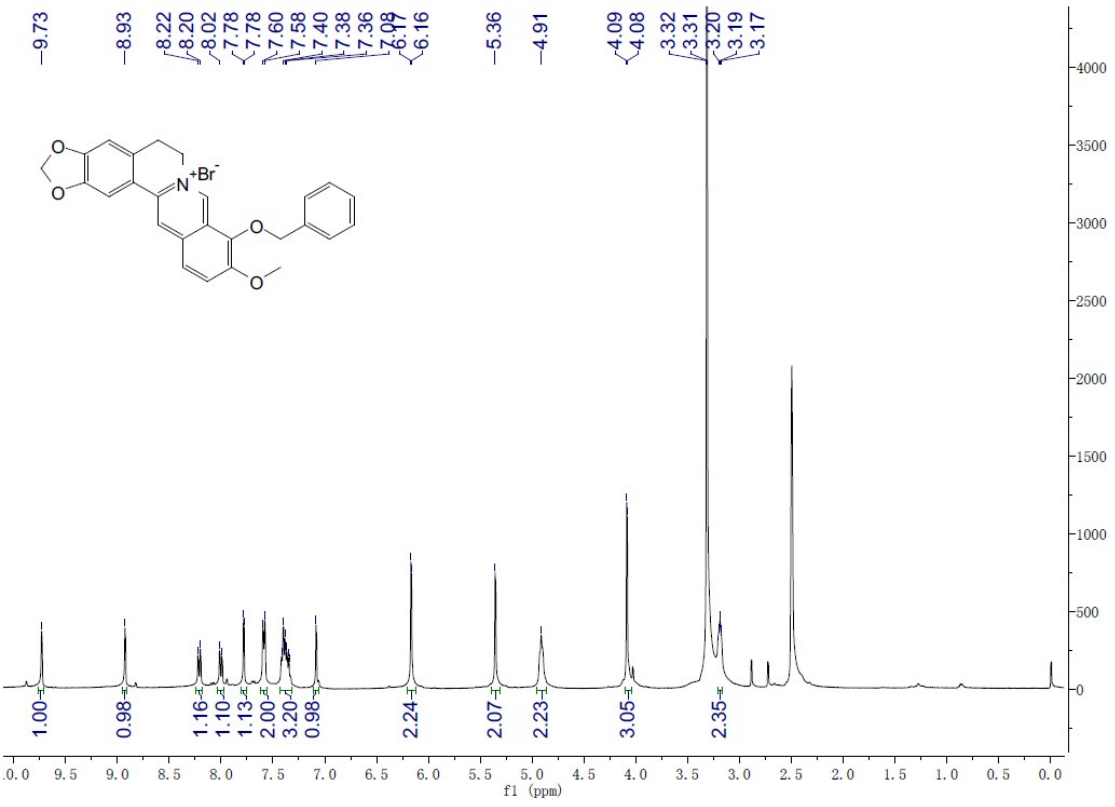

Fig.10. ^{1}H NMR, 9-*O*-benzyl-berberine (**3e**)

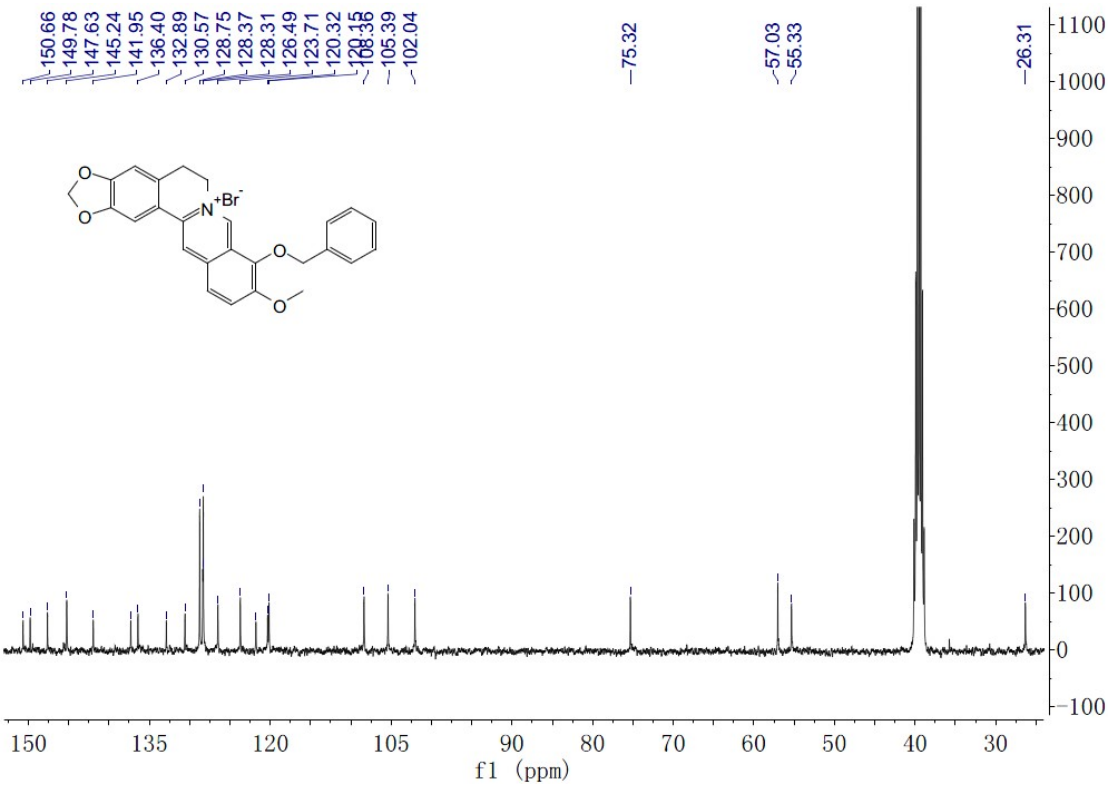

Fig.11. ^{13}C NMR, 9-*O*-benzyl-berberine (**3e**)

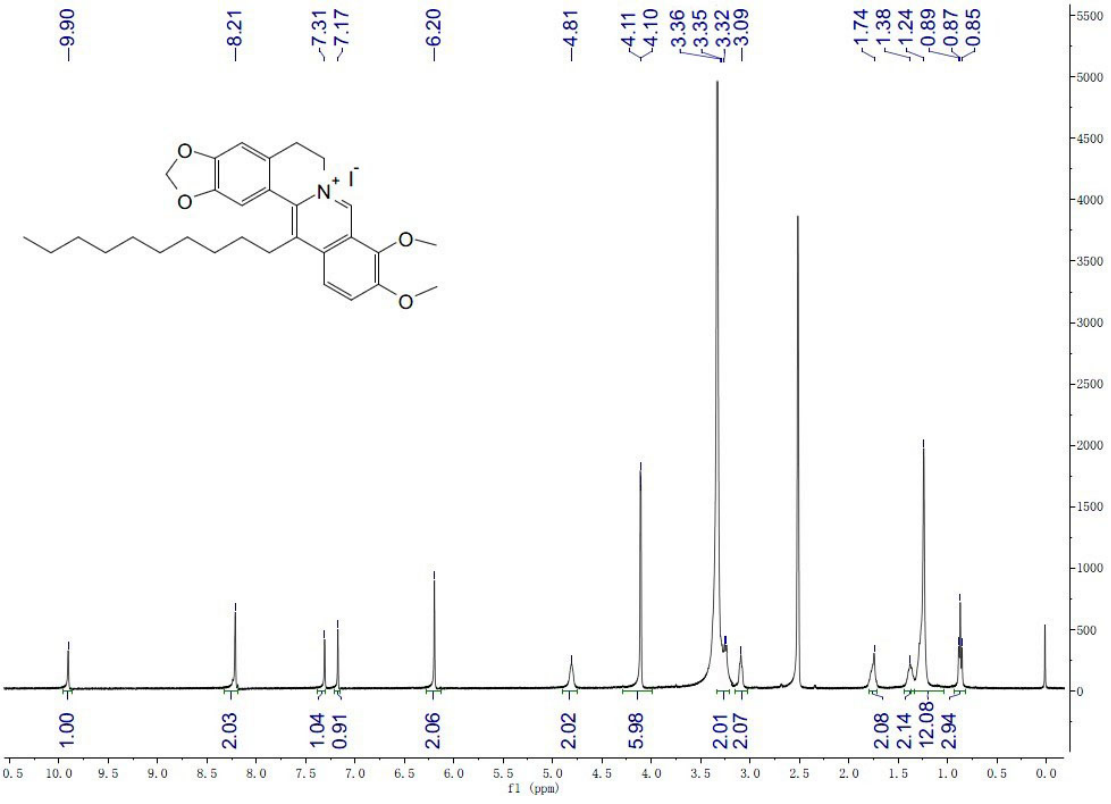

Fig.12. ^{1}H NMR, 13-decyl-berberine (**5f**)

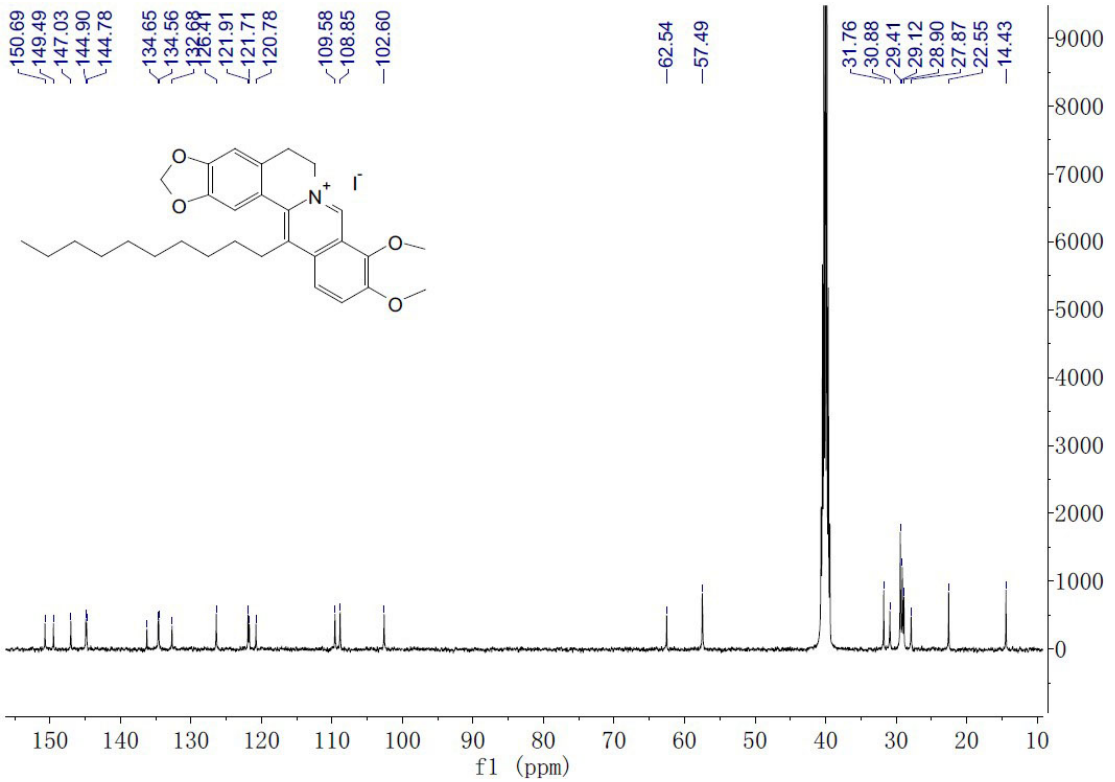

Fig.13. ^{13}C NMR, 13-decyl-berberine (**5f**)

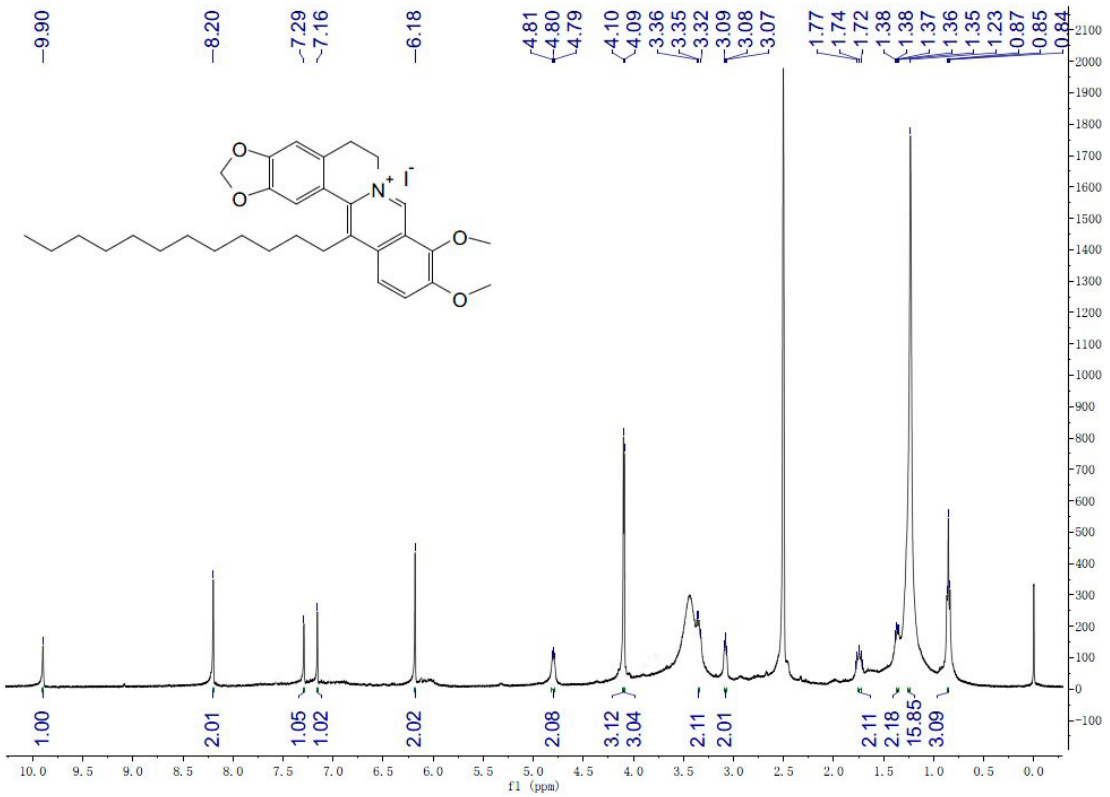

Fig.14. ^{1}H NMR, 13-dodecyl-berberine (**5g**)

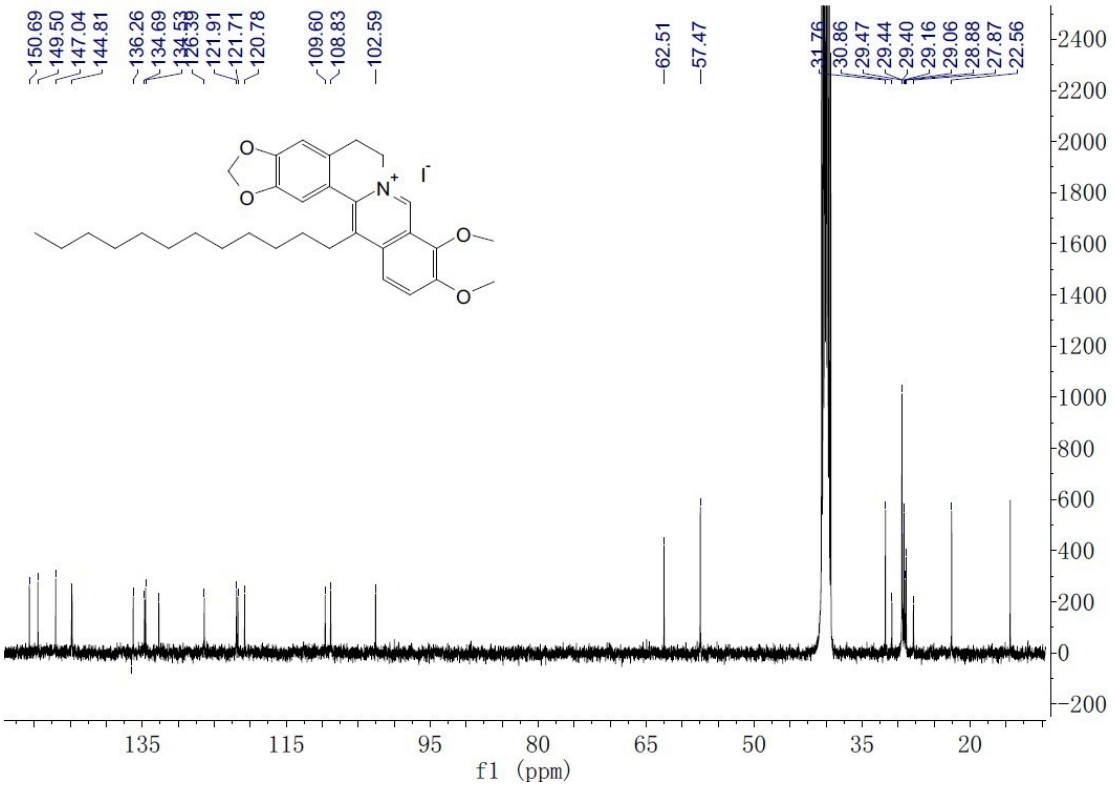

Fig.15. ^{13}C NMR,13-dodecyl-berberine (**5g**)

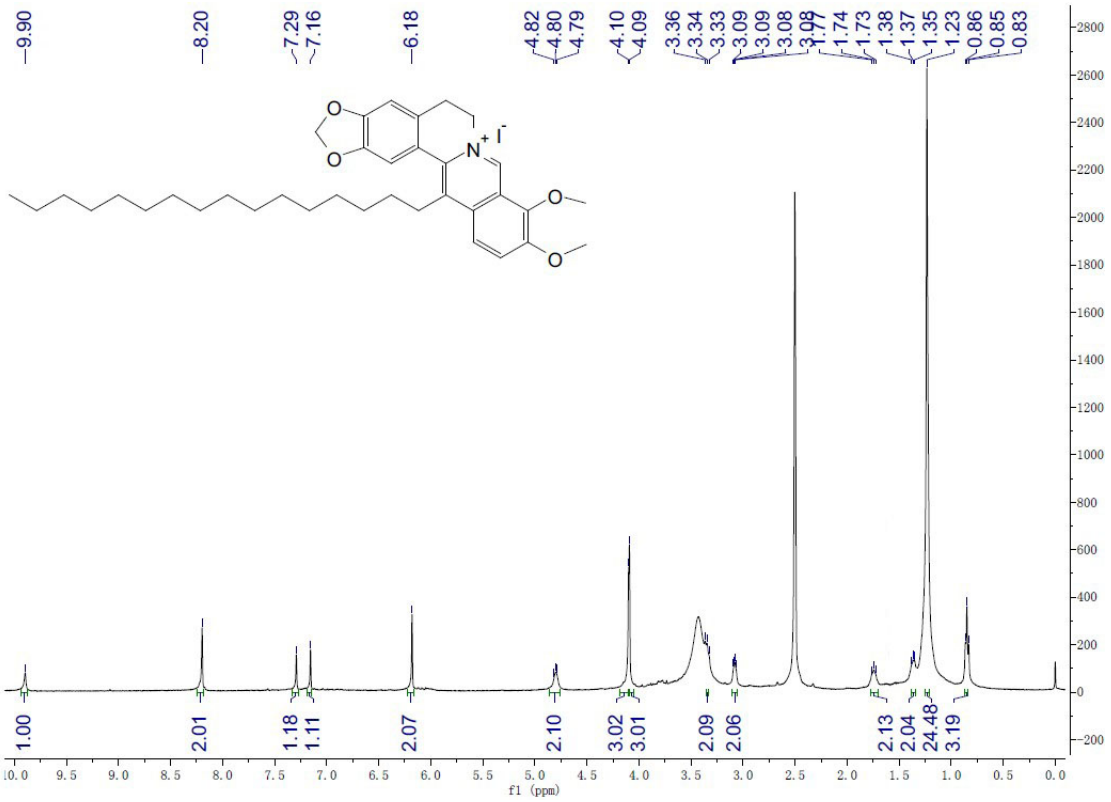

Fig.16. ^{1}H NMR, 13-cetyl-berberine (**5h**)

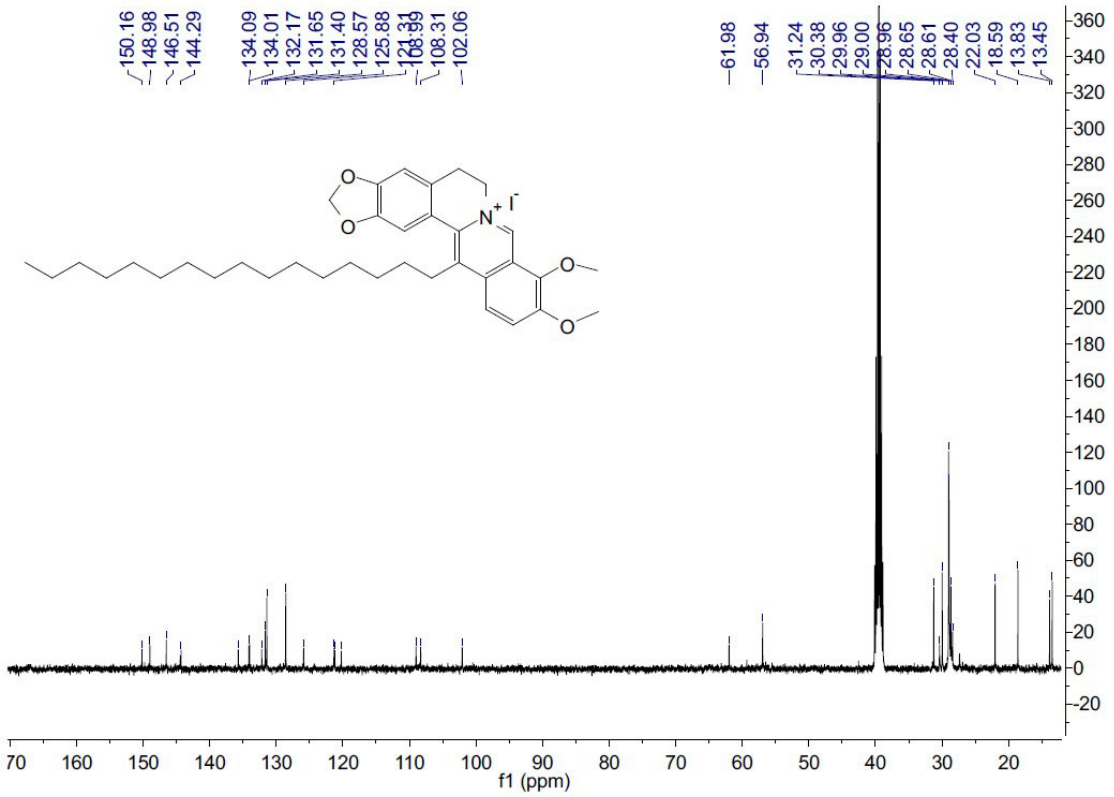

Fig.17. ^{13}C NMR, 13-cetyl-berberine (**5h**)

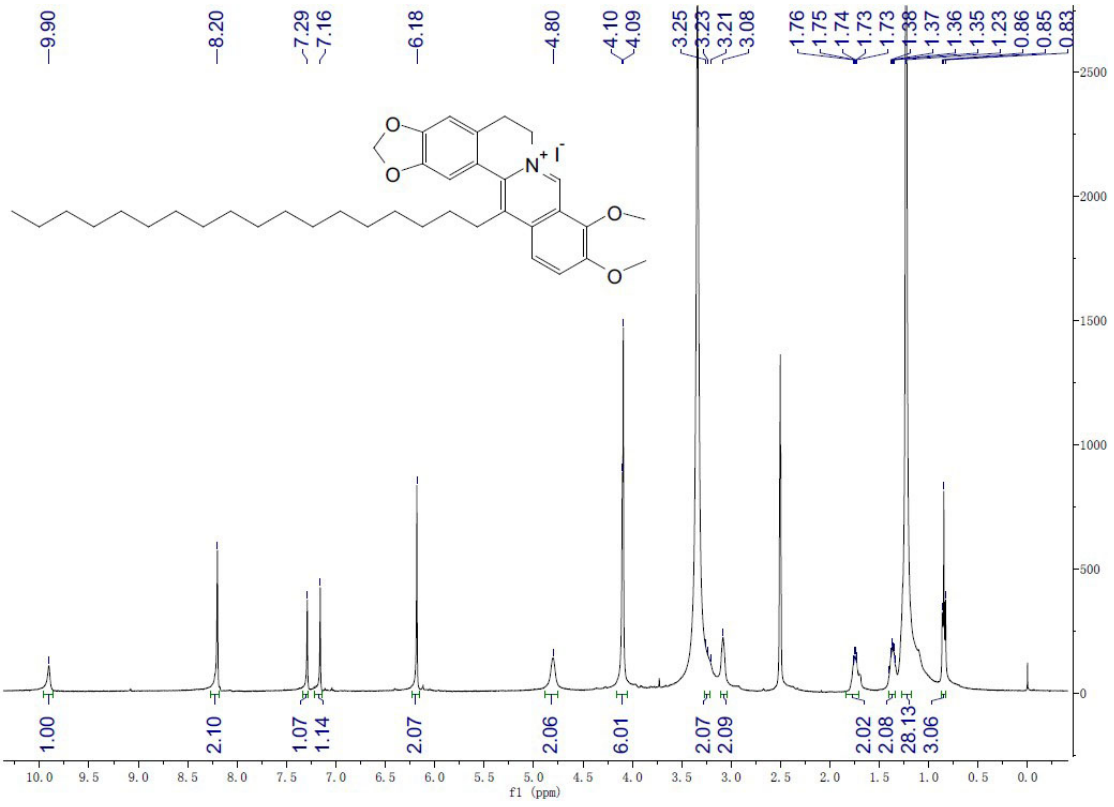

Fig.18. ^{1}H NMR, 13-octadecyl-berberine (**5i**)

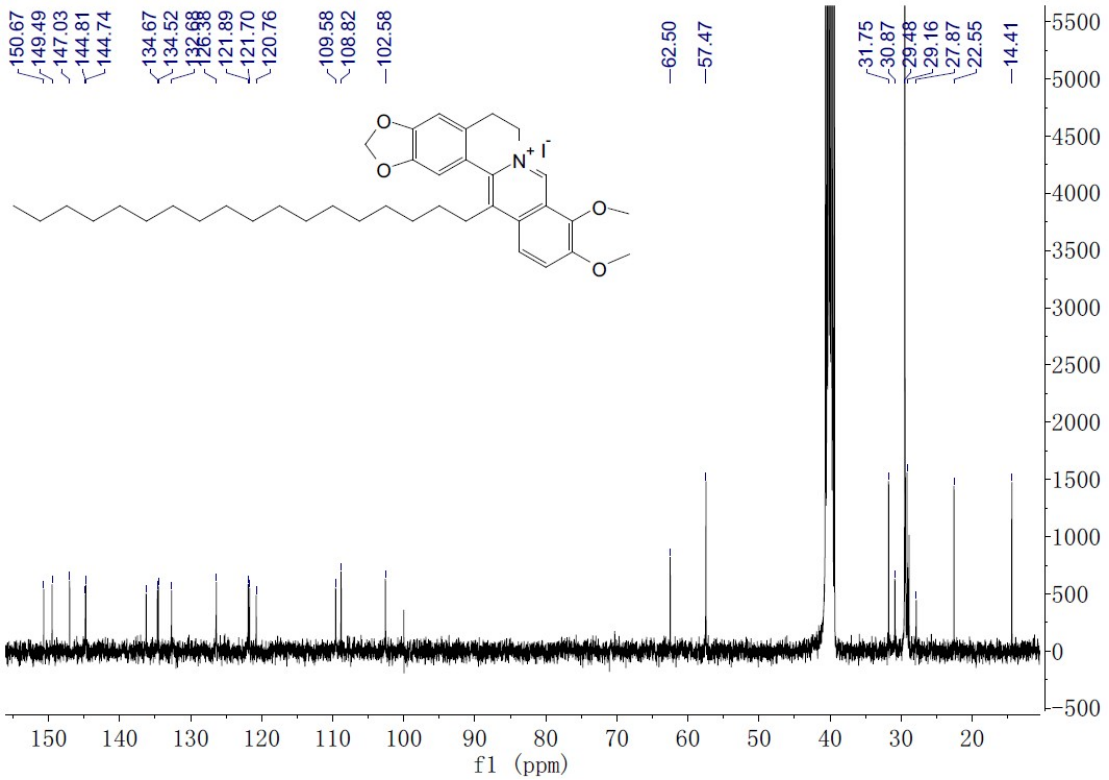

Fig.19. ^{13}C NMR, 13-octadecyl-berberine (**5i**)

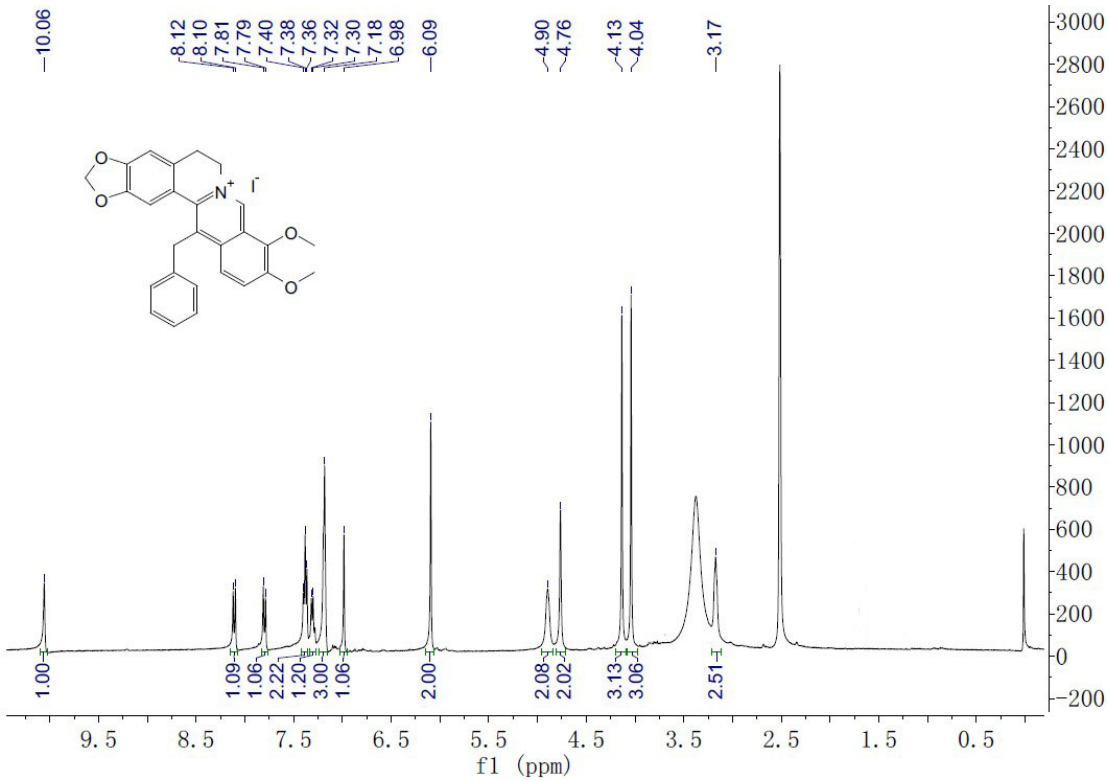

Fig.20. ^{1}H NMR, 13-benzyl-berberine (**5j**)

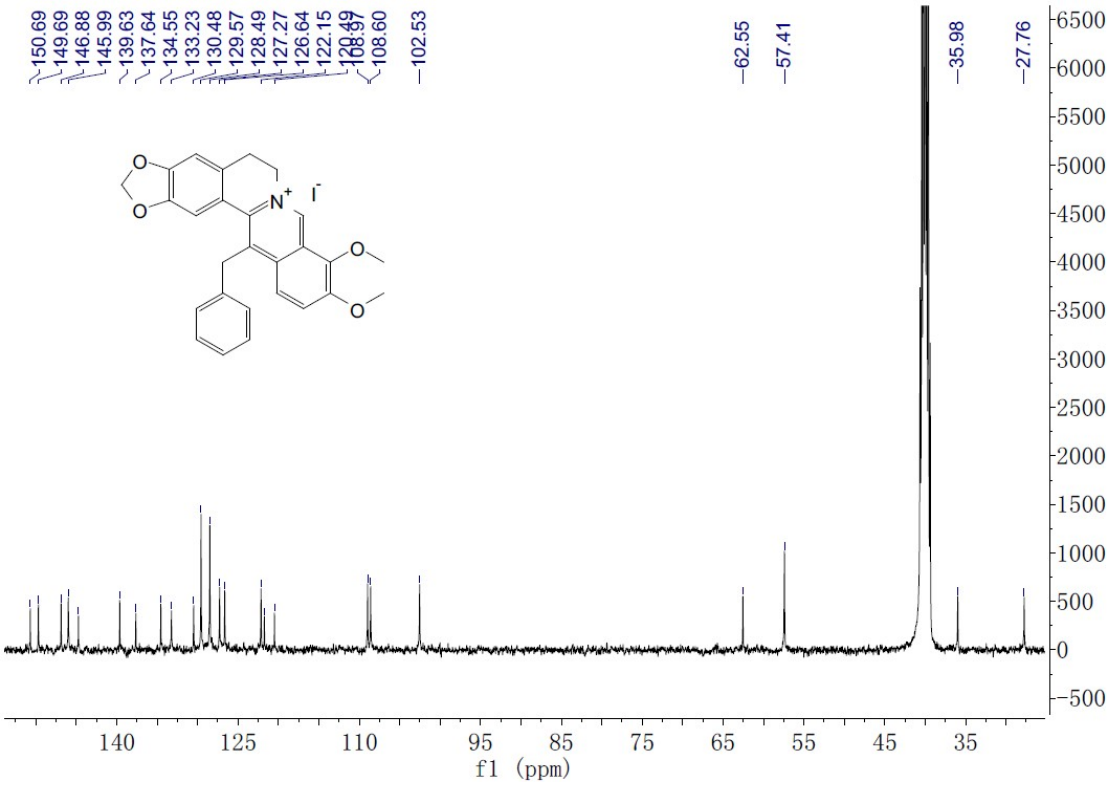

Fig.21. ^{13}C NMR, 13-benzyl-berberine (**5j**)

3. Mass spectra of compounds **1**, **3a-e** and **5f-j**.

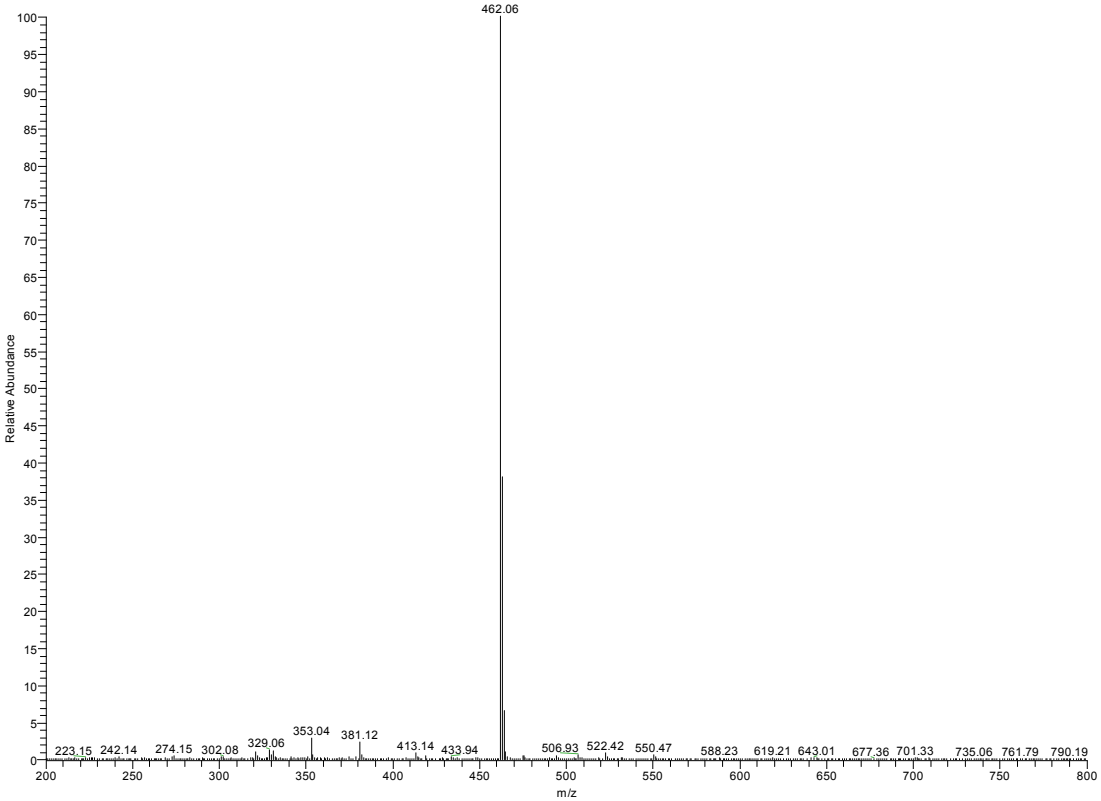

Fig.22. MS-ESI, 9-*O*-decyl-berberine (**3a**)

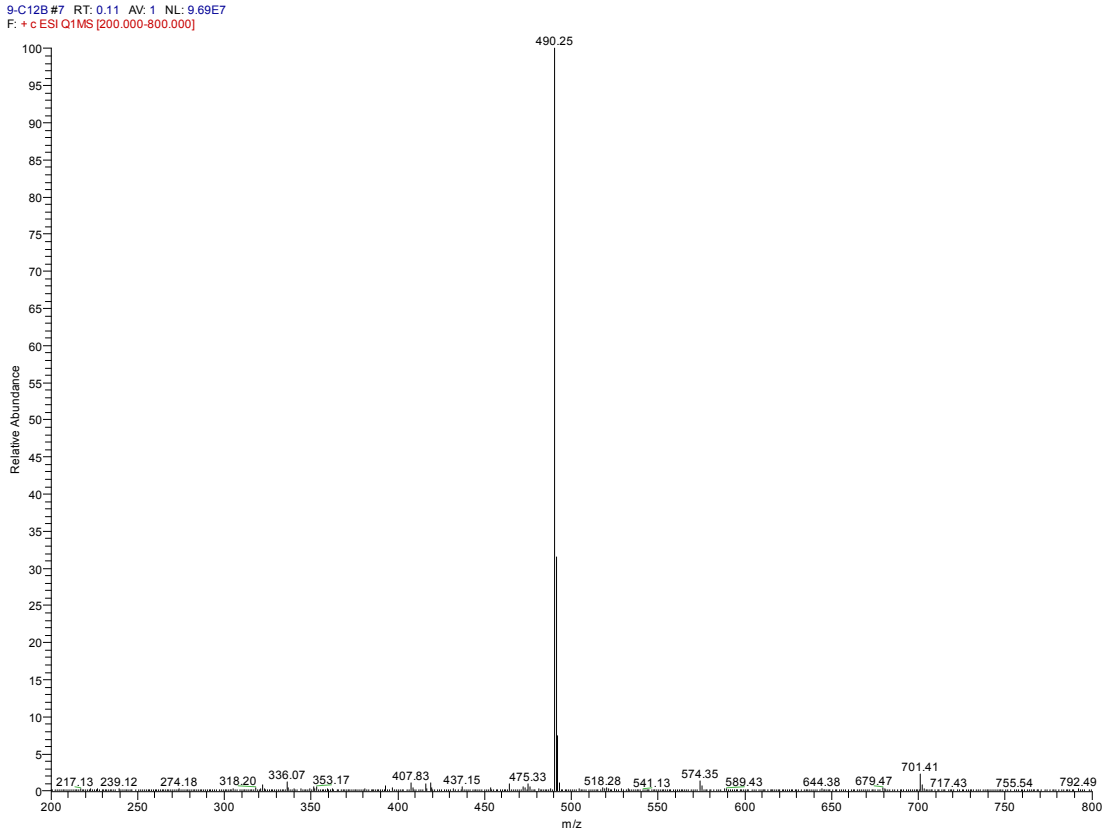

Fig.23. MS-ESI, 9-*O*-dodecyl-berberine (**3b**)

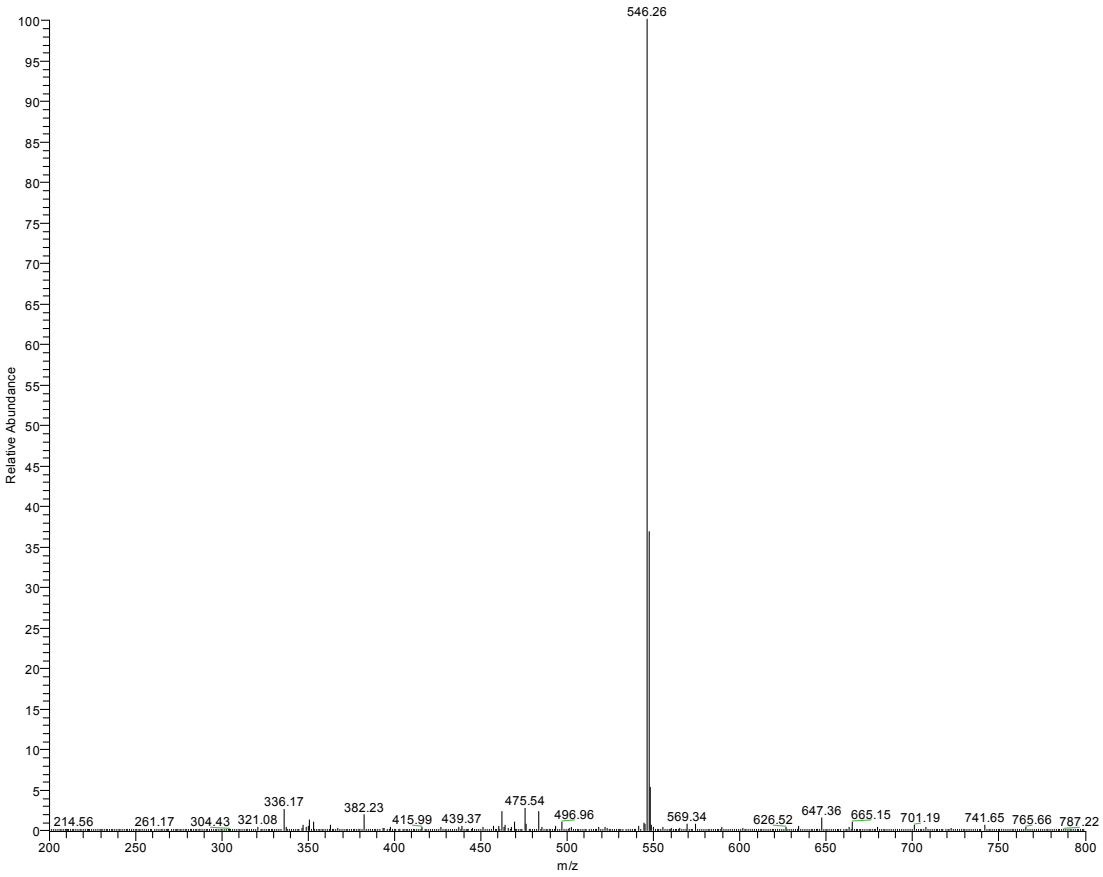

Fig.24. MS-ESI, 9-*O*-cetyl-berberine (**3c**)

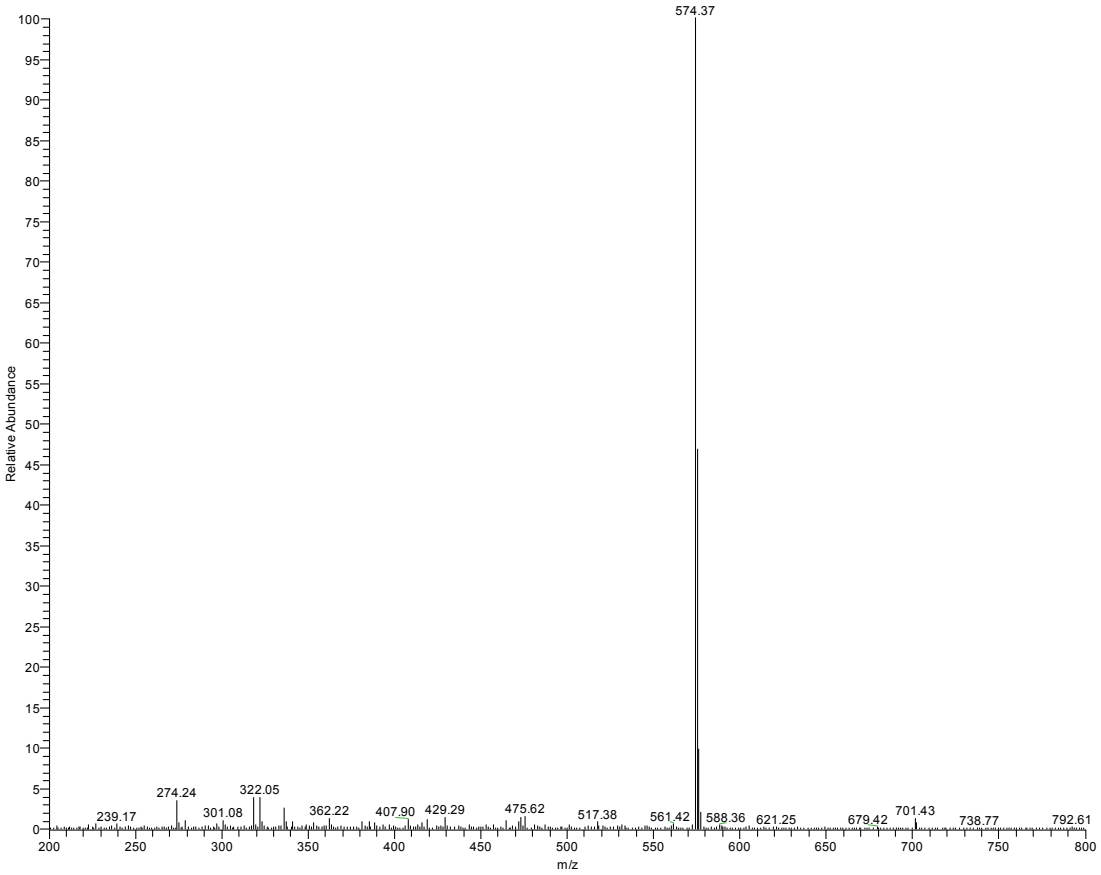

Fig.25. MS-ESI, 9-*O*-octadecyl-berberine (**3d**)

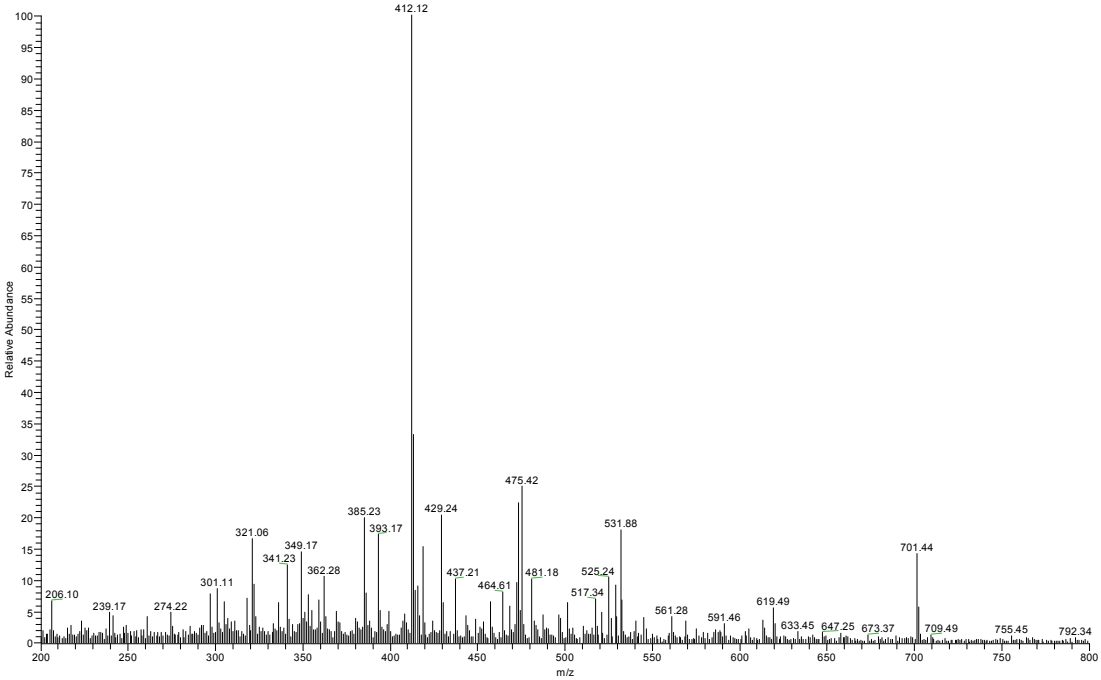

Fig.26. MS-ESI, 9-*O*-benzyl-berberine (**3e**)

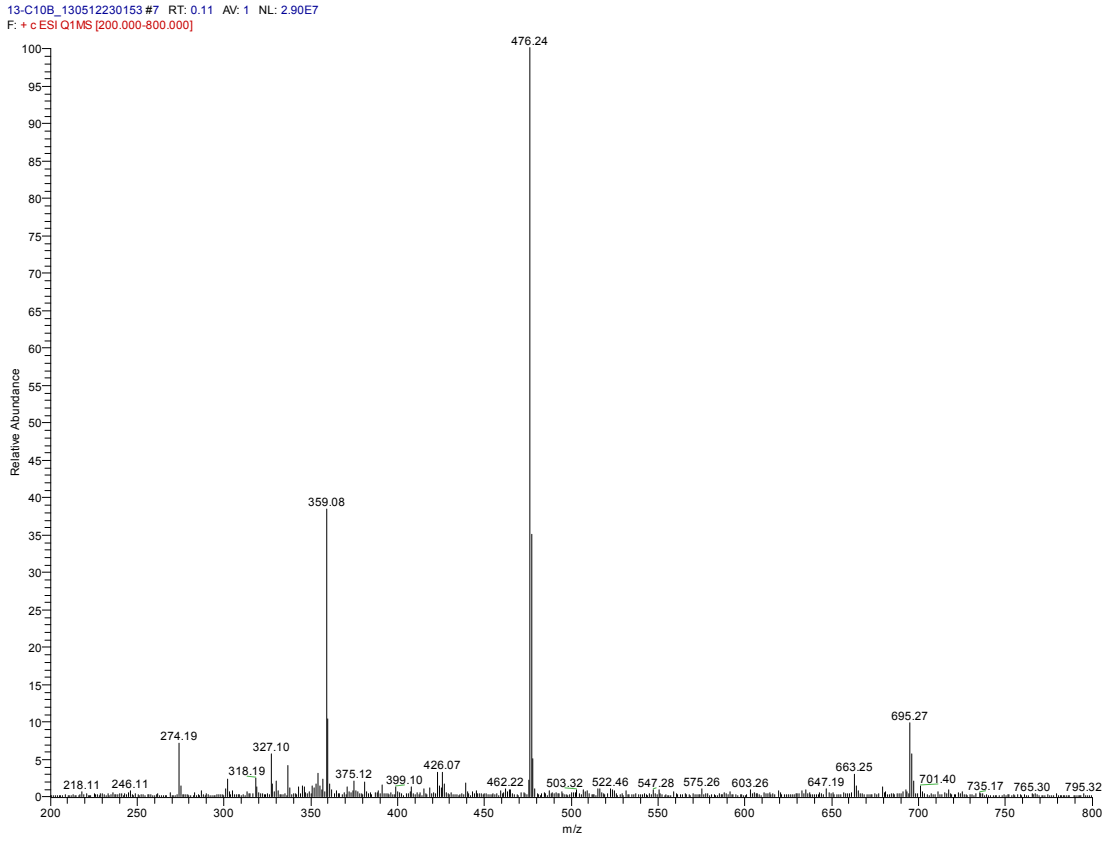

Fig.27. MS-ESI, 13-decyl-berberine (**5f**)

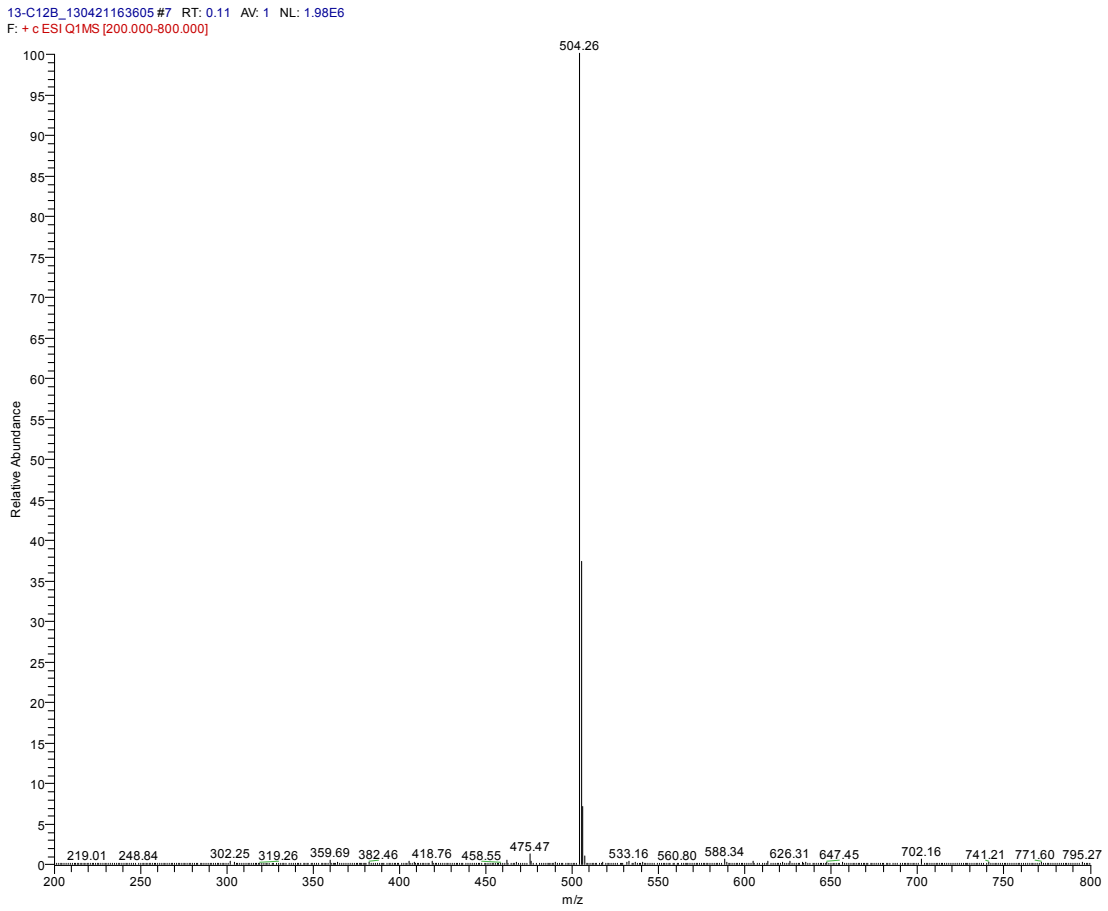

Fig.28. MS-ESI, 13-dodecyl-berberine (**5g**)

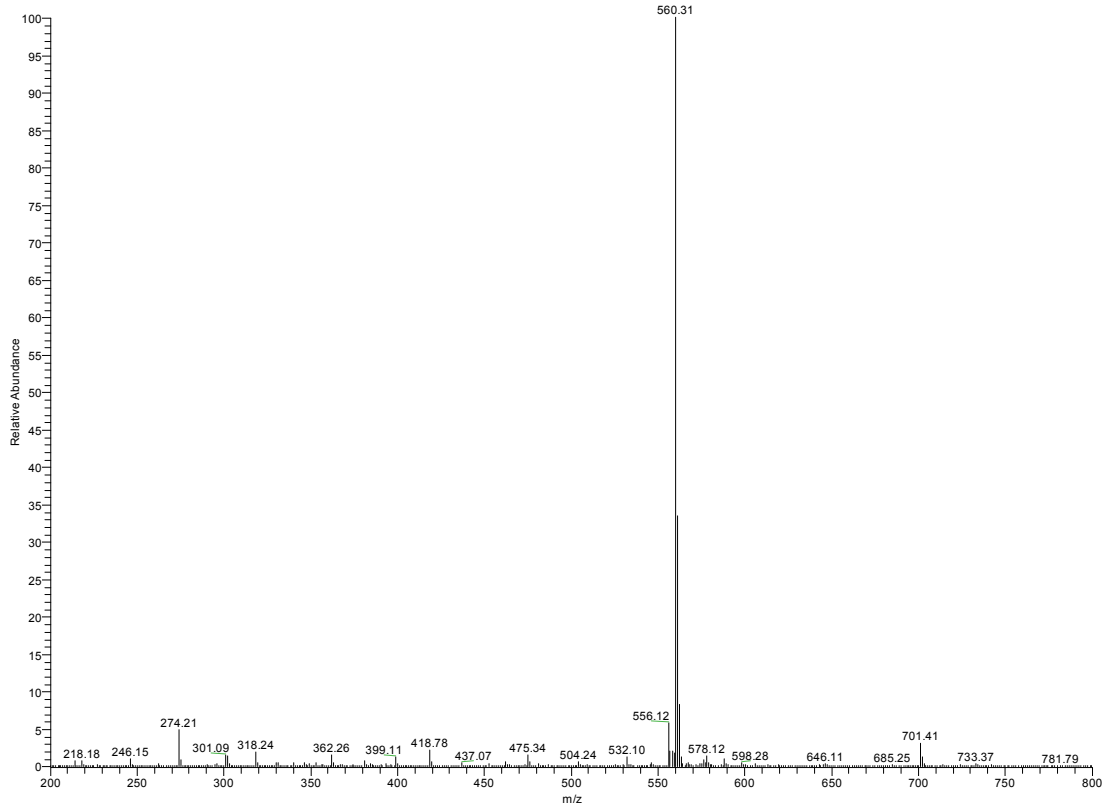

Fig.29. MS-ESI, 13-cetyl-berberine (**5h**)

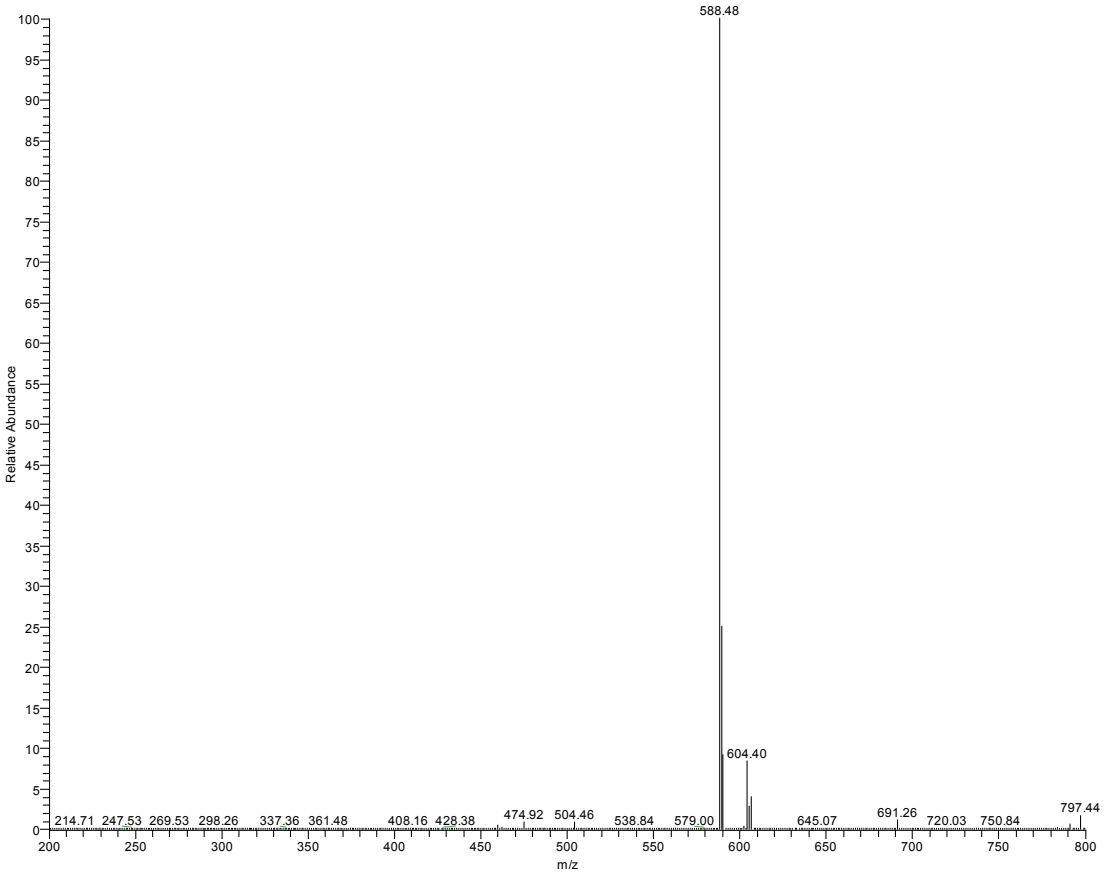

Fig.30. MS-ESI, 13-octadecyl-berberine (**5i**)

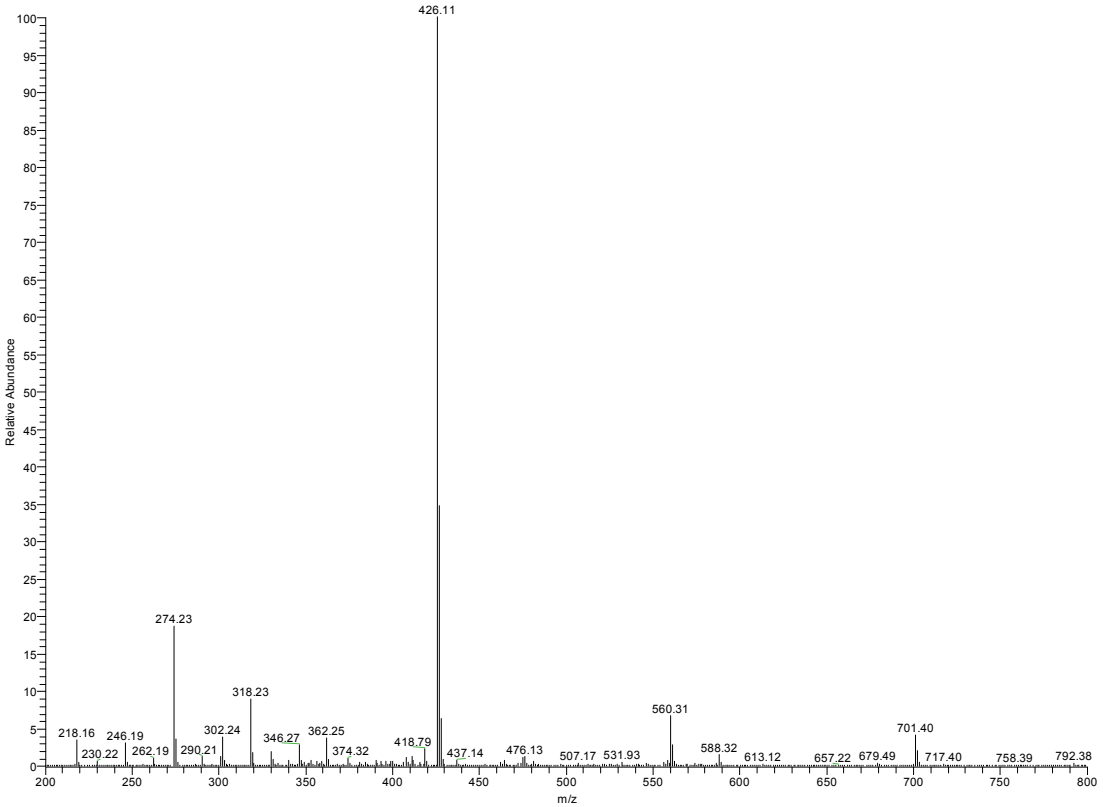

Fig.31. MS-ESI, 13-benzyl-berberine (**5j**)

4. Fluorescent spectra of compounds **1**, **3a-e** and **5f-j**.

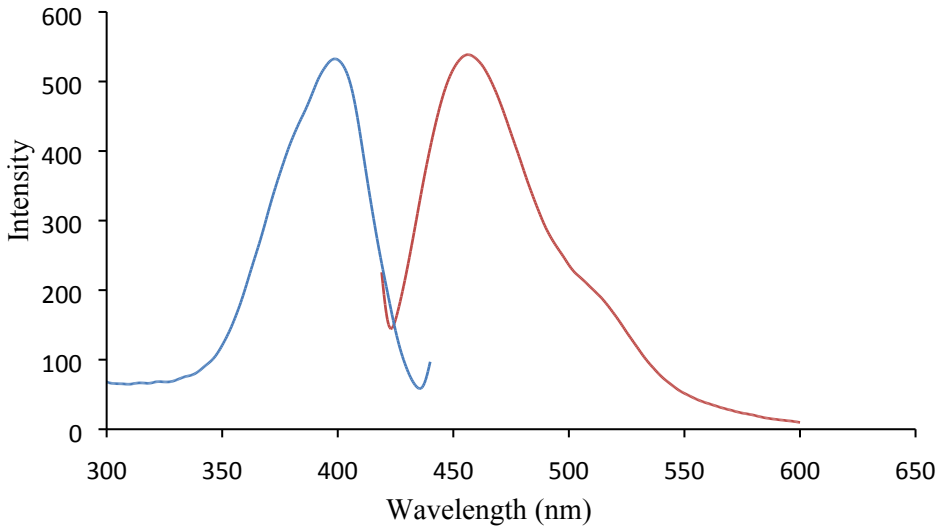

Fig.32. The fluorescent spectrum of berberine (**1**). Excitation, 399 nm; Emission, 460 nm.

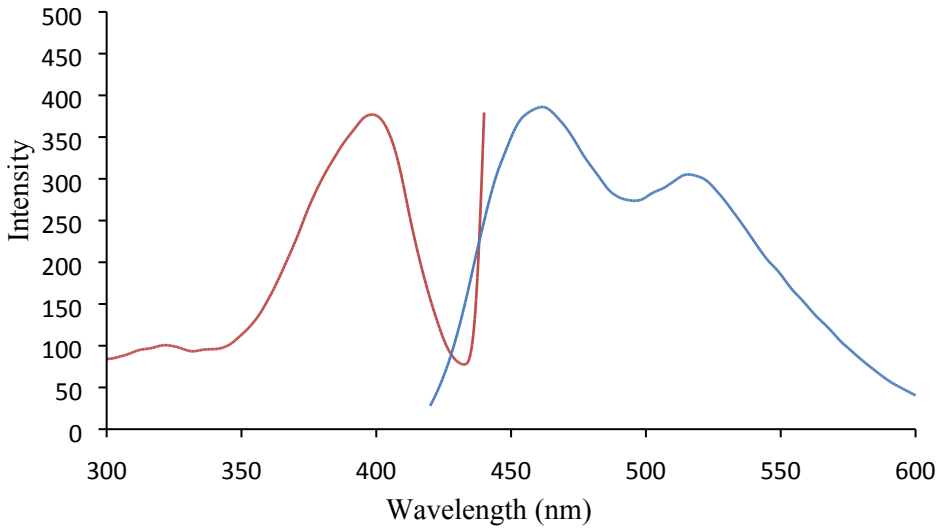

Fig.33. The fluorescent spectrum of 9-*O*-decyl-berberine (**3a**). Excitation, 399 nm; Emission, 460, 521 nm.

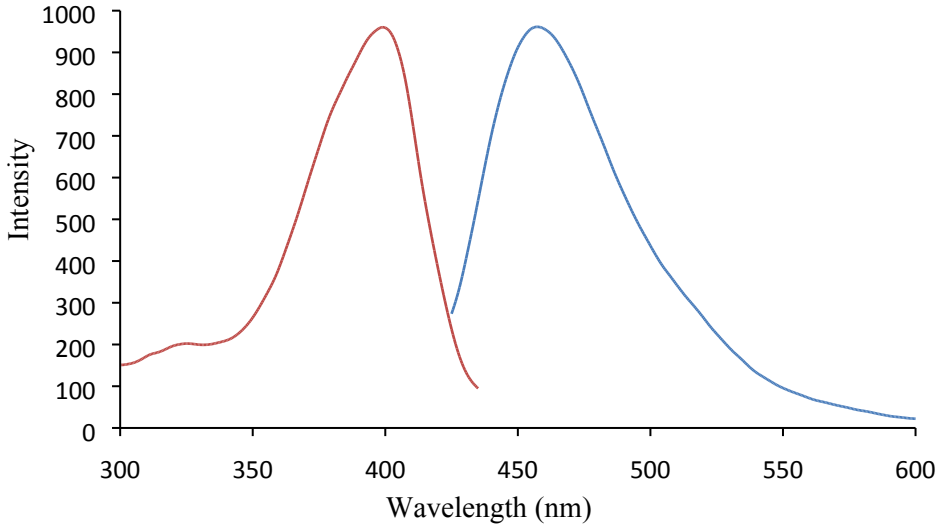

Fig.34. The fluorescent spectrum of 9-*O*-dodecyl-berberine (**3b**). Excitation, 400 nm; Emission, 456 nm.

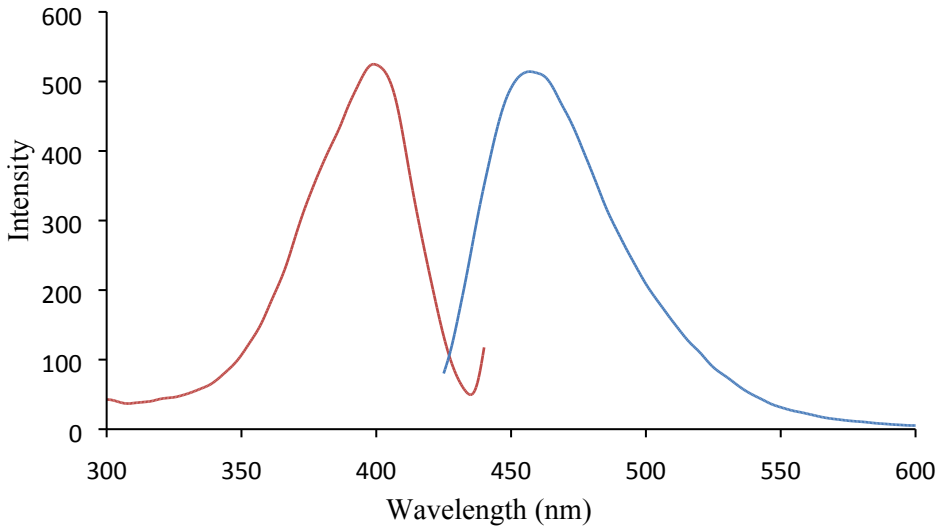

Fig.35. The fluorescent spectrum of 9-*O*-cetyl-berberine (**3c**). Excitation, 399 nm; Emission, 457 nm.

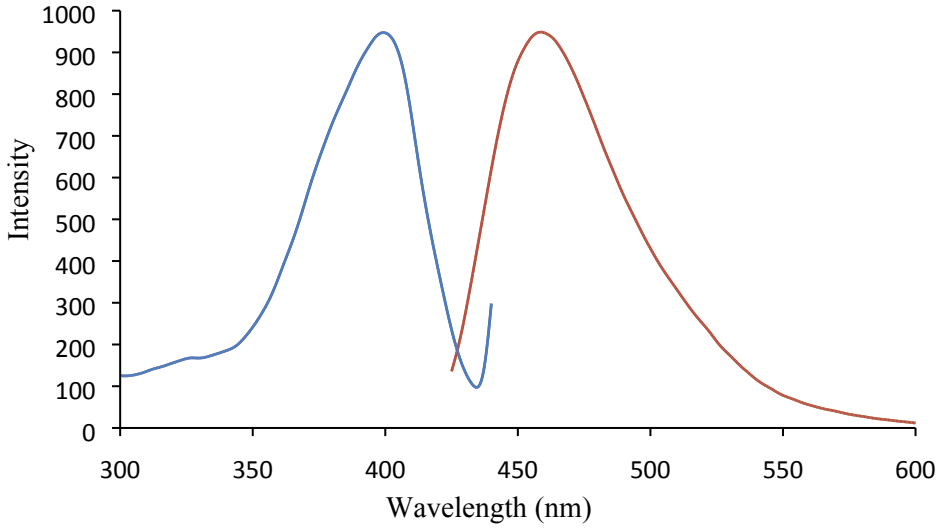

Fig.36. The fluorescent spectrum of 9-*O*-octadecyl-berberine (**3d**). Excitation, 399 nm; Emission, 459 nm.

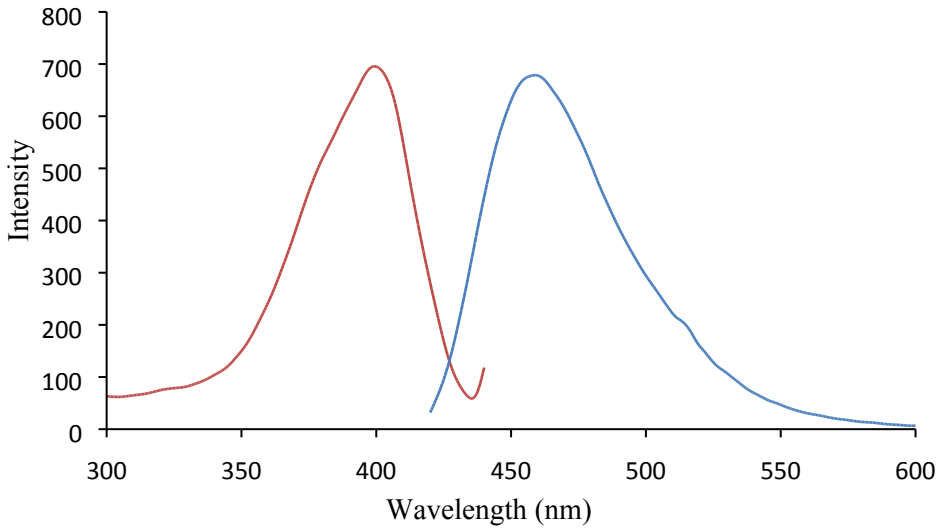

Fig.37. The fluorescent spectrum of 9-*O*-benzyl-berberine (**3e**). Excitation, 399 nm; Emission, 458 nm.

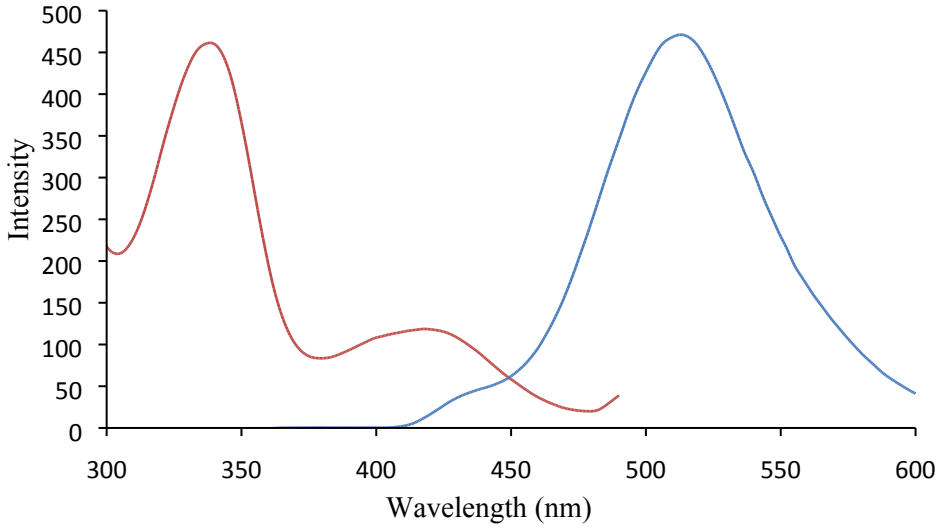

Fig.38. The fluorescent spectrum of 13-decyl-berberine (**5f**). Excitation, 343, 419 nm; Emission, 511 nm.

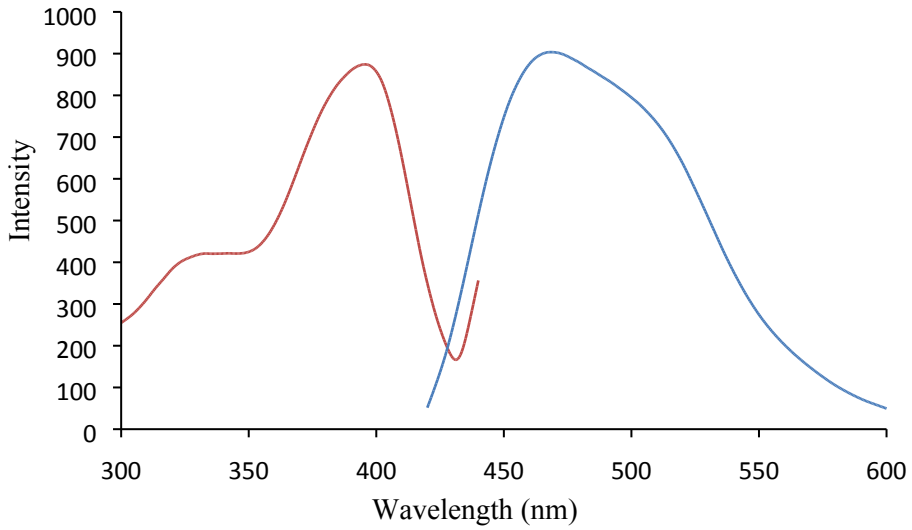

Fig.39. The fluorescent spectrum of 13-dodecyl-berberine (**5g**). Excitation, 398 nm; Emission, 466 nm.

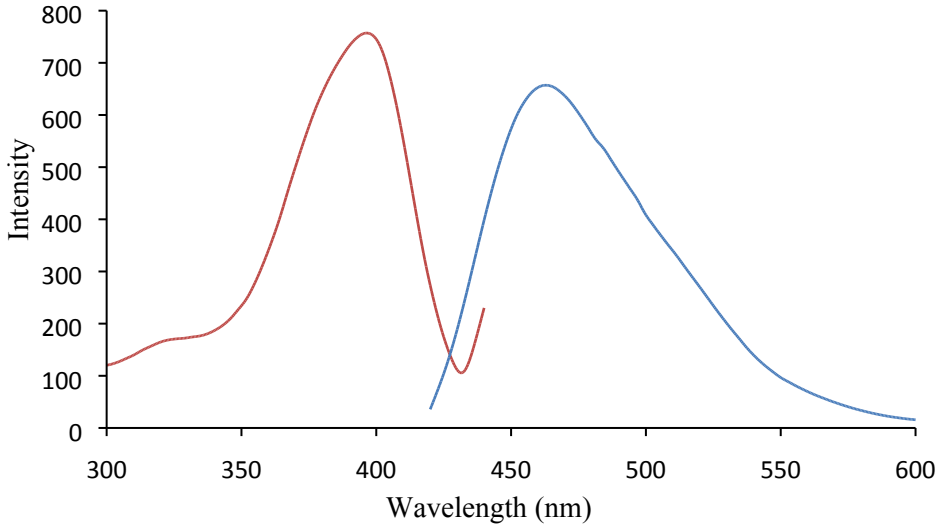

Fig.40. The fluorescent spectrum of 13-cetyl-berberine (**5h**). Excitation, 397 nm; Emission, 462 nm.

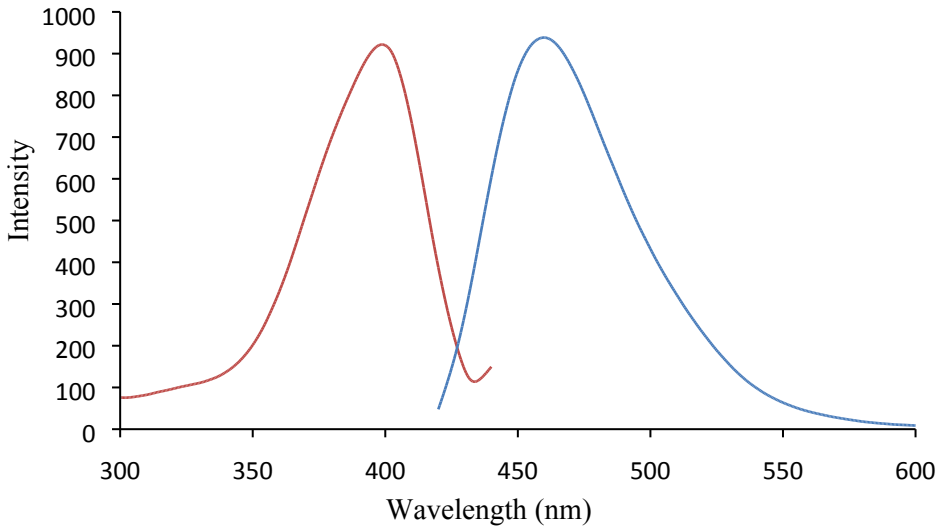

Fig.41. The fluorescent spectrum of 13-octadecyl-berberine (**5i**). Excitation, 399 nm; Emission, 459 nm.

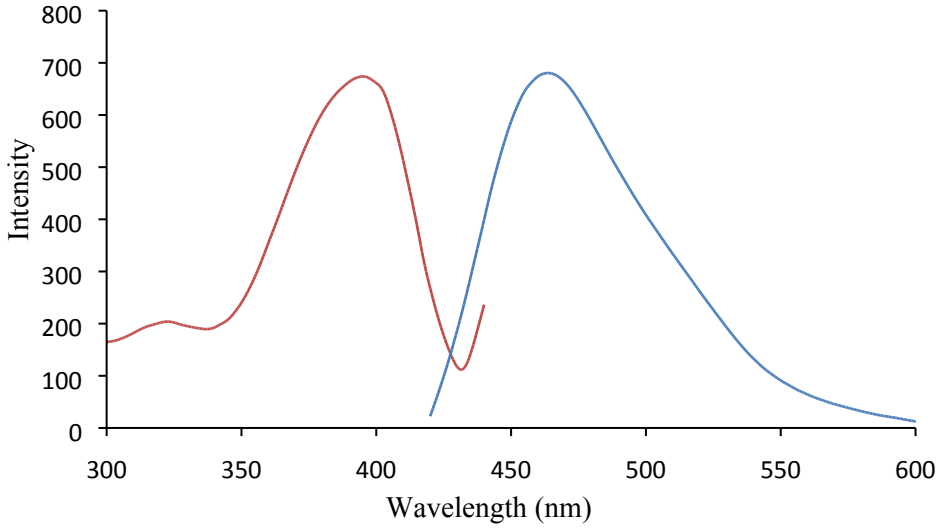

Fig.42. The fluorescent spectrum of 13-benzyl-berberine (**5j**). Excitation, 398 nm; Emission, 460 nm.

5. Ultraviolet spectra of compounds **1**, **3a-e** and **5f-j**.

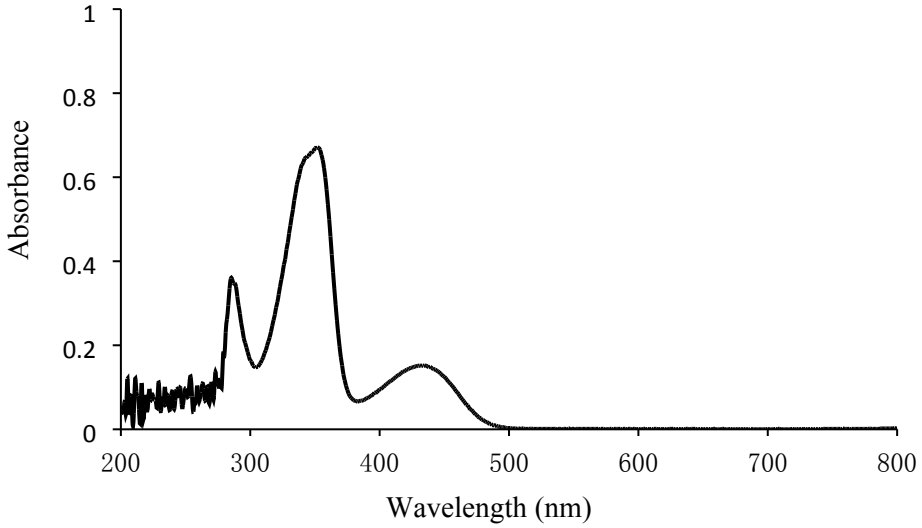

Fig. 43. The ultraviolet spectrum of berberine (**1**). Wavelength of maximum absorption (nm), 285, 352, 433.

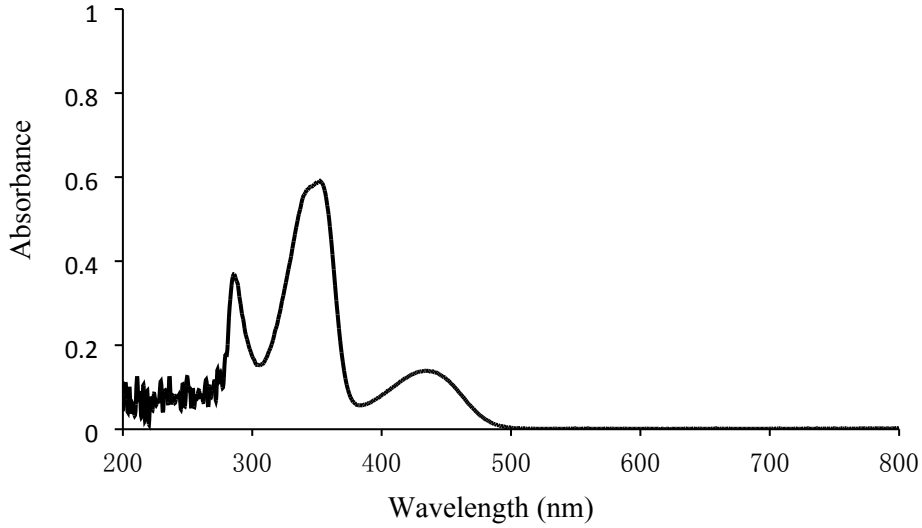

Fig. 44. The ultraviolet spectrum of 9-*O*-decyl-berberine (**3a**). Wavelength of maximum absorption (nm), 286, 352, 436.

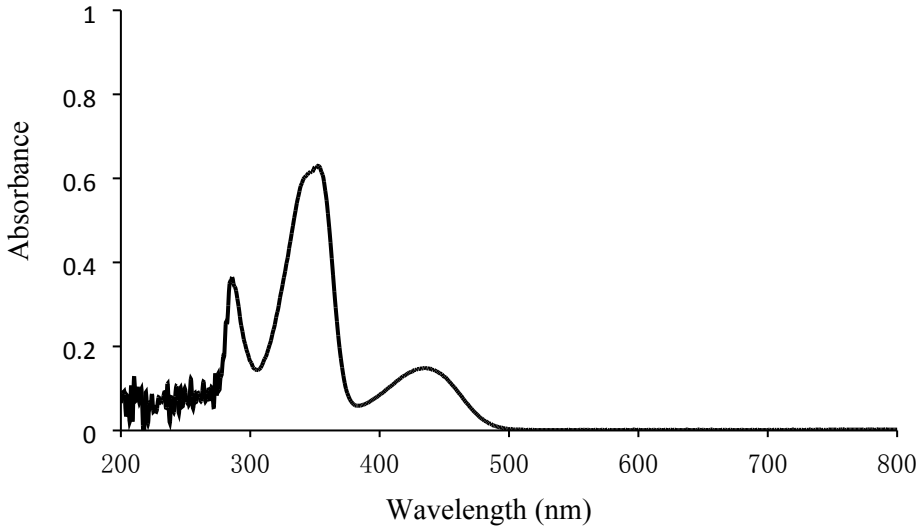

Fig. 45. The ultraviolet spectrum of 9-*O*-dodecyl-berberine (**3b**). Wavelength of maximum absorption (nm), 286, 353, 435.

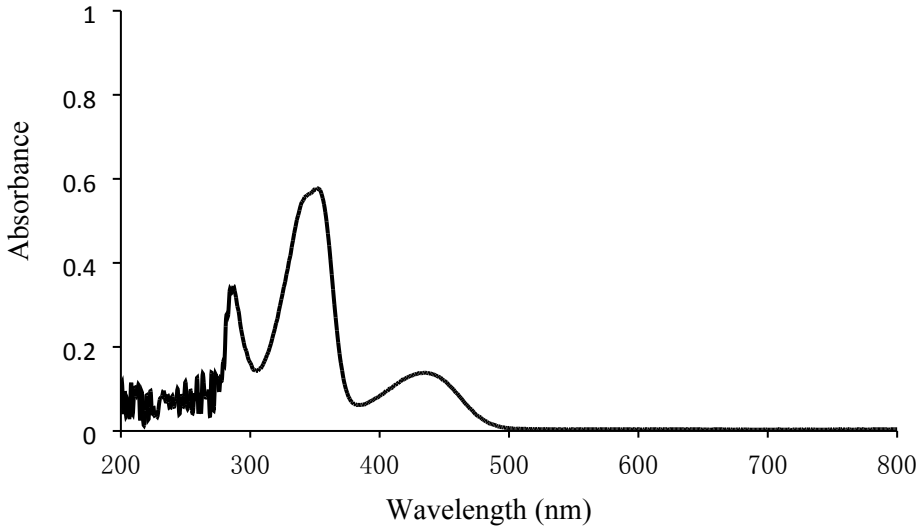

Fig. 46. The ultraviolet spectrum of 9-*O*-cetyl-berberine (**3c**). Wavelength of maximum absorption (nm), 287, 352, 435.

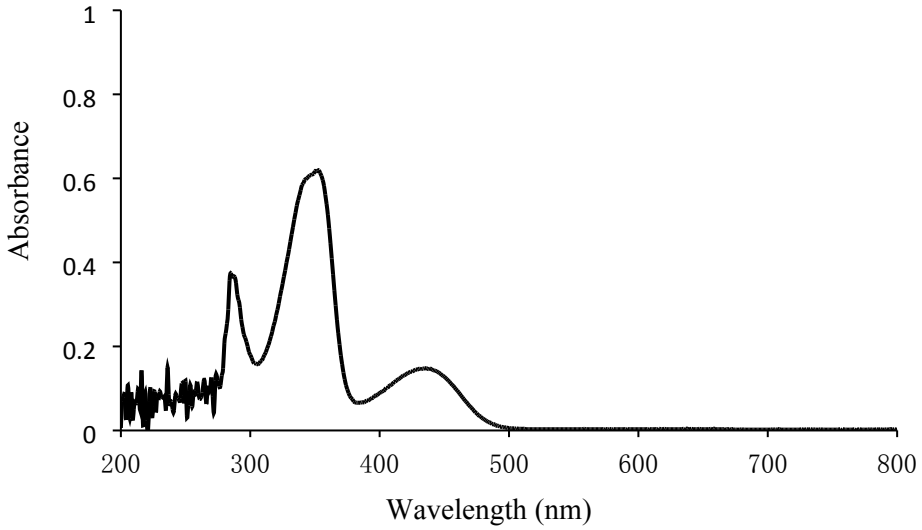

Fig. 47. The ultraviolet spectrum of 9-*O*-octacyl-berberine (**3d**). Wavelength of maximum absorption (nm), 285, 353, 436.

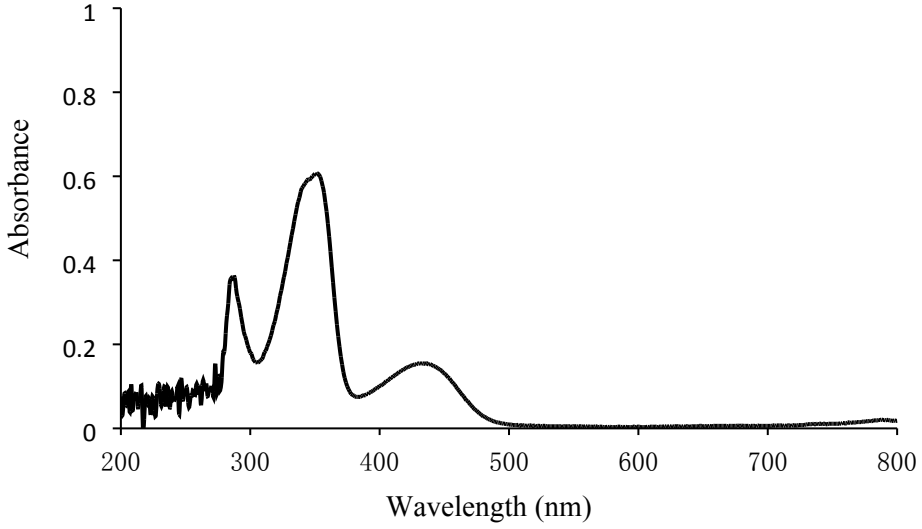

Fig. 48. The ultraviolet spectrum of 9-*O*-benzyl-berberine (**3e**). Wavelength of maximum absorption (nm), 288, 350, 436.

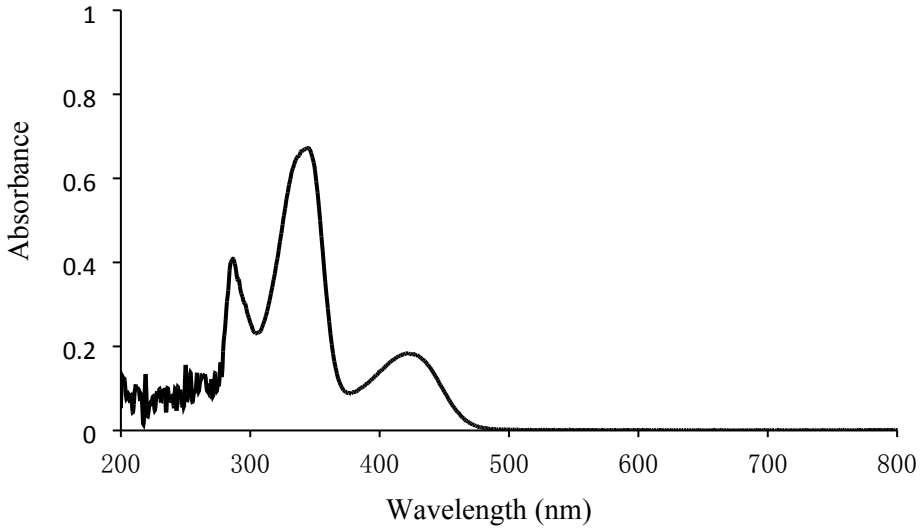

Fig. 49. The ultraviolet spectrum of 13-decyl-berberine (**5f**). Wavelength of maximum absorption (nm), 287, 345, 422.

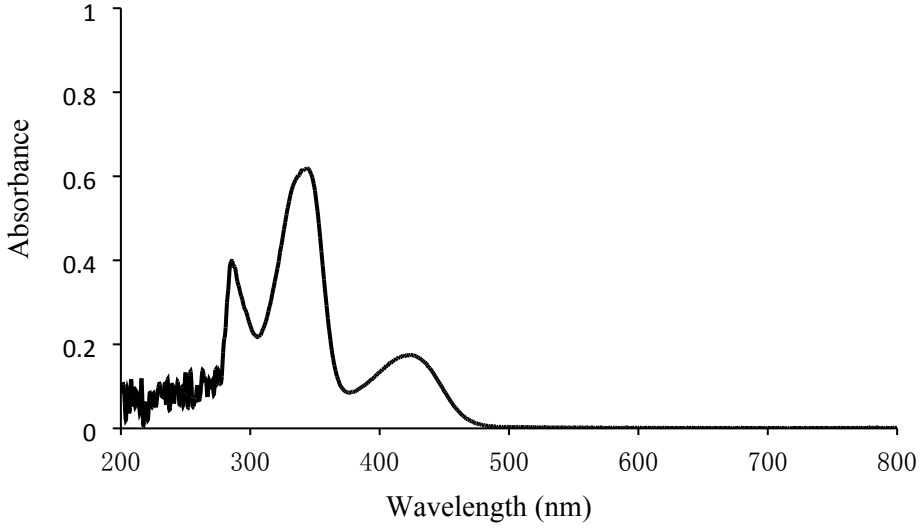

Fig. 50. The ultraviolet spectrum of 13-dodecyl-berberine (**5g**). Wavelength of maximum absorption (nm), 286, 344, 424.

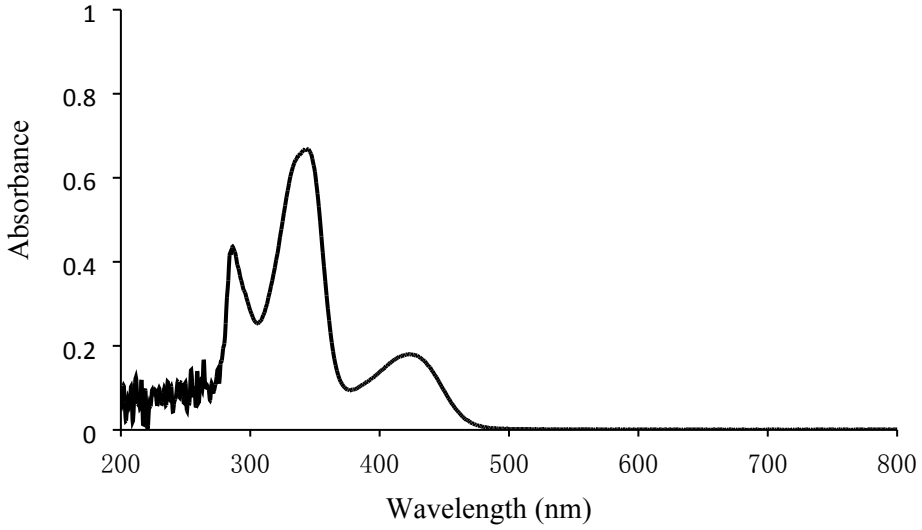

Fig. 51. The ultraviolet spectrum of 13-cetyl-berberine (**5h**). Wavelength of maximum absorption (nm), 286, 345, 423.

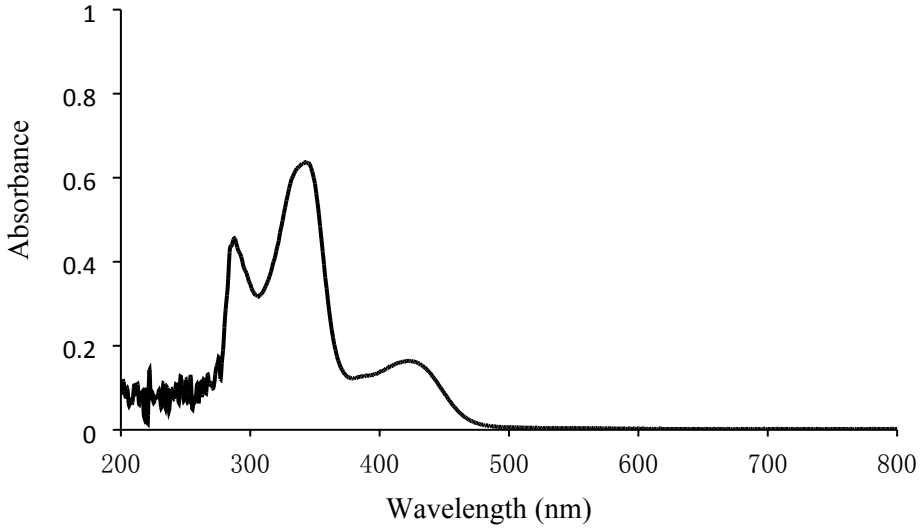

Fig. 53. The ultraviolet spectrum of 13-octadecyl-berberine (**5i**). Wavelength of maximum absorption (nm), 288, 343, 421.

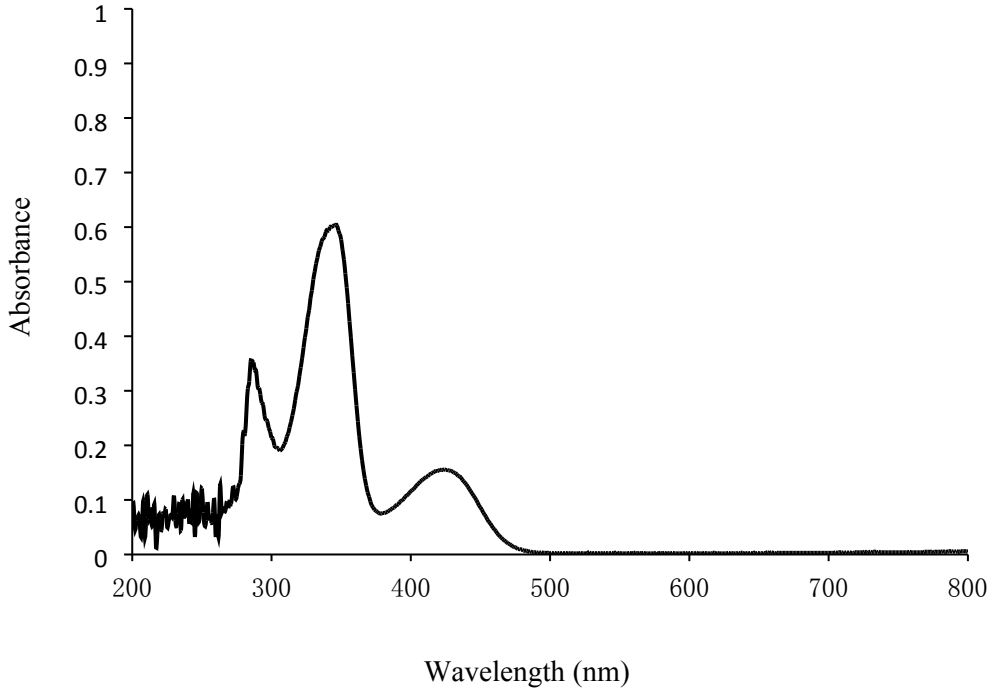

Fig. 53. The ultraviolet spectrum of 13-benzyl-berberine (**5j**). Wavelength of maximum absorption (nm), 287, 346, 424.